Exact, approximate, and hybrid treatments of viscous Rayleigh-Taylor and Richtmyer-Meshkov instabilities

Karnig O. Mikaelian
Lawrence Livermore National Laboratory, Livermore, California 94551, USA

(Received 6 November 2018; published 25 February 2019)

We consider Rayleigh-Taylor and Richtmyer-Meshkov instabilities at the interface between two fluids, one or both of which may be viscous. We derive exact analytic expressions for the amplitude $\eta(t)$ in the linear regime when only one of the fluids is viscous. The more general case is solved numerically using Laplace transforms. We compare the exact solutions of the initial-value problem with the approximate solutions of the eigenvalue problem used in a simple expression for $\eta(t)$ in terms of two growth rates, γ_+ and γ_-. We then propose a hybrid model as an improvement on the approximate model. The hybrid model is based on the same expression for $\eta(t)$ in terms of $\gamma_\pm$ but uses exact eigenvalues for γ_+, the larger growth rate, and a relationship between γ_- and γ_+. We also discuss two concepts: isogrowth wave number pairs and asymptotic decay. The first relies on viscosity in one or both fluids to identify perturbations of two different wavelengths having the same γ_+. The second concept, which is more general, can be found in viscous as well as inviscid fluids and requires only a specific initial growth rate $\dot\eta_0^{\rm critical}$ to force $\eta(t)\to 0$ as $t\to\infty$. We present several examples illustrating these two concepts and comparing exact, approximate, and hybrid treatments.

DOI: 10.1103/PhysRevE.99.023112

I. INTRODUCTION, MOTIVATION, AND BACKGROUND

Hydrodynamic instabilities are known to cause the growth, often exponential, of small perturbations at an interface between two fluids, leading to transition from laminar to turbulent flow. The Rayleigh-Taylor (RT) instability arises when a low-density fluid supports a higher-density fluid in a gravitational field [1], or accelerates it with or without the presence of gravity [2]. The Richtmyer-Meshkov (RM) instability arises when a shock wave passes through the interface, in either direction [3,4]. Recent interest in RT and RM instabilities stems from their effect on inertial-confinement fusion (ICF) [5–7] and supernova explosions [8]. A six-volume review by Zhou citing numerous recent experimental, theoretical, and numerical investigations can be found in [9,10].

In this paper we consider RT and RM instabilities in two-fluid systems when one or both of the fluids are viscous. We present exact, approximate, and "hybrid" (combining exact and approximate) expressions for the evolution of perturbations at the interface between the two fluids. Viscosity almost always slows down the growth and has important applications in a number of fields: ferrofluids [11], tectonics [12], ICF [13], exploding foils [14], aerobreakup [15], and astrophysics [16].

Linear analyses start with a small-amplitude, initial value η_0, sinusoidal perturbation $\eta_0\cos(kx)$ of wavelength $\lambda = 2\pi/k$ in the x direction, taking the acceleration or the shock to be in the y direction. We shall consider only two-dimensional (2D) planar geometry. For the perturbation amplitude $\eta(t)$ to remain in the linear regime it must satisfy $\eta(t)k \ll 1$.

Since the Navier-Stokes (NS) equations are second order in time their solutions, in the linear regime, must have the form

$$\eta(t) = \eta_0 F(t) + \dot\eta_0 G(t), \tag{1}$$

where $\dot\eta_0 \equiv \dot\eta(t=0) \equiv (\frac{d\eta}{dt})_0$. F and G satisfy initial conditions $F(0) = \dot G(0) = 1$ and $G(0) = \dot F(0) = 0$. We shall refer to Eq. (1) as the initial-value (IV) solution.

In Eq. (1) we suppress the dependence of F and G on the parameters of the problem: ρ_1, ρ_2, μ_1, μ_2, g and/or ΔV, $T^{(s)}$, and k, where ρ = density, μ = viscosity, g = acceleration, ΔV = interfacevelocity jump following a shock, and $T^{(s)}$ is the surface tension at the interface. Of course these parameters determine the stability or instability of the configuration, taken to be two infinitely thick fluids (finite-thickness effects will be considered elsewhere). Stability is determined by a growth rate γ which depends strongly on those parameters. Following Chandrasekhar [17], γ is determined by assuming that $\eta(t) \sim e^{\gamma t}$ in the linearized NS equations. This yields an eigenvalue problem with γ the eigenvalue, and the resulting equation that determines γ is often called the "dispersion relation" (DR). Assuming that there are two solutions denoted, for example, by γ_+ and γ_-, we proposed [18]

$$\eta(t) = \eta_0 \frac{\gamma_+ e^{\gamma_- t} - \gamma_- e^{\gamma_+ t}}{\gamma_+ - \gamma_-} + \dot\eta_0 \frac{e^{\gamma_+ t} - e^{\gamma_- t}}{\gamma_+ - \gamma_-}, \tag{2}$$

from which $F(t)$ and $G(t)$ can be readily identified. All seven or eight parameters defining the system appear only in $\gamma_\pm$ and a real, large γ_+ indicates a highly unstable system as $\eta(t) \sim e^{\gamma_+ t}$. We shall refer to Eq. (2) as the eigenvalue (EV) solution.

The exact solution for $\eta(t)$ is given by the IV solution, assuming that the linearized, time-dependent NS equations have been solved exactly. The EV solution, Eq. (2), is only an approximation, more of an ansatz. The two solutions may or may not agree with each other, depending on the complexity of the problem—they will agree if the fluids are inviscid, but not if one or both of them are viscous.

A somewhat subtle point, which had escaped us when we proposed Eq. (2), is what to do when there is only one eigenvalue, say γ_+. We hope to provide an answer in this paper by proposing a hybrid solution. This was not an issue in our earlier work [18] because we had coupled Eq. (2) with another approximation, that of using approximate $\gamma_\pm$, making our results doubly approximate justified only by their simplicity.

In anticipation of what is to follow in this paper we simply state that the hybrid model uses Eq. (2) with γ_+ calculated from the exact DR and $\gamma_- = -gkA/\gamma_+$, where A is the usual Atwood number defined as $(\rho_2 - \rho_1)/(\rho_2 + \rho_1)$.

Interestingly, finding a hybrid solution lies on the following general observation: The instability of a system, evidenced by the existence of a large and positive γ_+, means that perturbations *in general* will grow with time. It does not mean that *every* perturbation will grow—it depends on the initial conditions. Assume that the ratio $F(\infty)/G(\infty)$ exists and is finite, and define

$$\dot{\eta}_0^{\text{critical}} \equiv -\eta_0 \lim_{t\to\infty}[F(t)/G(t)]. \tag{3}$$

If $\dot{\eta}_0 = \dot{\eta}_0^{\text{critical}}$ then $\eta(t) = \eta_0[F(t) - (\frac{F(\infty)}{G(\infty)})G(t)] \to 0$ as $t \to \infty$. In this process, which we label "asymptotic decay," the η_0 and $\dot{\eta}_0$ terms in Eq. (1) "cancel" each other out asymptotically even though each term separately grows large. If Eq. (2) applies then we need to zero out the coefficient of the growing $e^{\gamma_+ t}$ term which is $(\dot{\eta}_0 - \eta_0\gamma_-)/(\gamma_+ - \gamma_-)$. Hence

$$\dot{\eta}_0^{\text{critical}} = \gamma_-\eta_0 \,(\text{approximate}). \tag{4}$$

In this paper we will propose using the concept of a critical $\dot{\eta}_0$ to define a γ_- where one does not exist or is not allowed by the DR.

In most early applications of the RT instability $\dot{\eta}_0$ was set equal to zero, a natural choice. With the relatively recent focus on RM instabilities [7,9,10,19] we know that each shock is accompanied by a change in $\dot{\eta}$, the growth rate of the perturbation. The concept of a critical $\dot{\eta}_0$ and asymptotic decay, occurring in RT instabilities, is similar but somewhat different from that of freeze-out occurring in RM instabilities [19] where a perturbation immediately stops growing ($\dot{\eta} = 0$) after a second shock tuned to cancel the growth induced by a first shock. In contrast, with asymptotic decay $\dot{\eta}_0^{\text{critical}}$ drives $\eta \to 0$ in an unstable system which otherwise would be growing exponentially with time. Examples will illustrate this point in Sec. IV. Note that this argument is quite general and does not require nor preclude viscosity.

We first review previous work starting with the classic system of two inviscid fluids [1]. The DR reads

$$\gamma^2 - gkA = 0, \tag{5}$$

from which $\gamma_\pm = \pm\gamma$ with $\gamma = \gamma^{\text{classical}} = \sqrt{gkA}$. In this paper we consider only unstable configurations $A > 0$ and $g \geqslant 0$. Equation (5) was derived first by Lord Rayleigh [1] for gravity. Substituting for $\gamma_\pm$ in Eq. (2) one obtains the well-known result for the classical RT instability:

$$\eta(t) = \eta_0 \cosh(\gamma t) + \frac{\dot{\eta}_0}{\gamma}\sinh(\gamma t),\ \gamma = \sqrt{gkA}. \tag{6}$$

Taylor used the IV approach to derive [2]

$$\ddot{\eta}(t) - gkA\eta(t) = 0, \tag{7}$$

whose solution, for a constant g, is the same as given above in Eq. (6).

We now review the classical RM problem. Richtmyer [3] first treated the shock as an instantaneous acceleration, essentially replacing g by $\Delta V\delta(t)$ in Eq. (7) [$\delta(t)$ is the Dirac delta function]. Integrating Eq. (7) once leads to

$$\dot{\eta}_0 = \Delta V kA\eta_0. \tag{8}$$

Assuming $g = 0$ after the shock one obtains

$$\eta(t) = \eta_0 + \dot{\eta}_0 t = \eta_0(1 + \Delta V kAt), \tag{9}$$

another well-known result for a single-shock RM instability.

If $g \neq 0$ after the shock one must combine RM and RT instabilities [18] by solving Eq. (7) with an initial $\dot{\eta}_0$ given by Eq. (8). If after the shock $g = $ const. then one simply uses the solution given by Eq. (6) in which $\dot{\eta}_0$ is given by Eq. (8). Note that the condition for criticality, $\dot{\eta}_0^{\text{critical}} = \gamma_-\eta_0 = -\gamma\eta_0 = -\eta_0\sqrt{gkA} = \Delta V kA\eta_0$, will be satisfied if $\Delta V = -\sqrt{\frac{g}{kA}}$. The negative sign means the initial shock must proceed from the heavy to the light fluid.

For double-shock freeze-out one generalizes Eq. (8) to read [19]

$$\dot{\eta}_{0+} = \Delta V kA\eta_0 + \dot{\eta}_{0-}, \tag{10}$$

where $\dot{\eta}_{0-}$ is set by the first shock arriving at some time $t < 0$ and the second shock arriving at $t = 0$. Clearly, the two terms on the right-hand side of the above equation can cancel each other out, leading to $\dot{\eta}_{0+} = 0$ after the second shock. Examples can be found in Ref. [19].

The above discussion is exact within the limitation of linearity, incompressibility, and $\mu_1 = \mu_2 = T^{(s)} = 0$. Finite surface tension can be accounted for by the replacement

$$g \to g - \frac{k^2 T^{(s)}}{\rho_2 - \rho_1}. \tag{11}$$

For simplicity of notation we will suppress surface tension terms remembering that in the final formulas the above replacement must be done if $T^{(s)}$ is appreciable. Its effect on the RM instability was treated in [18].

The problem, however, becomes extremely complex when we include viscosity, calling for approximate treatments which must be compared against the few cases where an exact treatment is possible, the main subject of this paper. Needless to say, all treatments must return to the above inviscid results for $\mu_1 = \mu_2 = 0$ (this is not as simple as it appears) but, in general, approximations must be used for viscous fluids. Suffice it to note that there are no explicit exact results for arbitrary μ_1 and μ_2. There are solutions for special cases and to differentiate one case from another we propose using a viscous Atwood number A_μ in analogy with the one based on density:

$$A_\mu \equiv \frac{\mu_2 - \mu_1}{\mu_2 + \mu_1}. \tag{12}$$

The first exact and general eigenvalue treatment was carried out by Harrison [17,20] followed by Bellman and Pennington [21], deriving a DR reproduced in our Appendix A. It cannot be solved explicitly for arbitrary A and A_μ and one must solve it numerically. An explicit analytic solution for the

simplest case of all, a single viscous fluid, was presented in Ref. [22] solving a quartic equation. This single-fluid case can be described as the case $A = 1$ and $A_\mu = 1$, which we refer to as case A. Most often studied [17] is case B where $\nu_1 \equiv \frac{\mu_1}{\rho_1} = \nu_2 \equiv \mu_2/\rho_2$; i.e., $A_\mu = A$, arbitrary A. Two cases which have not been studied very much are case C, $\mu_1 = 0$, and case D, $\mu_2 = 0$; the results are presented in this paper. The following summarize these four cases:

$$A_\mu = 1,\ A = 1\ \big(\text{single fluid}\big),\quad \text{case A}, \tag{13a}$$

$$A_\mu = A,\ A\ \text{ arbitrary},\quad \text{case B}, \tag{13b}$$

$$A_\mu = 1,\ A\ \text{ arbitrary},\quad \text{case C}, \tag{13c}$$

$$A_\mu = -1,\ A\ \text{ arbitrary},\quad \text{case D}. \tag{13d}$$

Of course the single-fluid case A can be considered as a special case of C where the "heavy" fluid has viscosity μ_2.

All four cases above share one common characteristic: Their DRs reduce to a fourth-order polynomial equation which can be solved explicitly [23], although numerical solutions are more common. With exact, explicit solutions in hand we will compare them with approximate techniques, which we discuss next. These are useful because of their simplicity.

The first approximate DR was proposed by Hide [24]:

$$\gamma^2 + 2\nu k^2 \gamma - gkA = 0, \tag{14}$$

where

$$\nu \equiv \frac{\mu_2 + \mu_1}{\rho_2 + \rho_1}. \tag{15}$$

The larger root of Eq. (14),

$$\gamma_+ = \gamma_+^{\text{approx.}} = -\nu k^2 + \sqrt{gkA + \nu^2 k^4}, \tag{16}$$

was shown earlier [21] to be an upper bound of the exact DR. Invariably, γ_+ has been shown to be a good approximation, not just an upper bound, to the exact result, and our comparison confirms this fact (see Fig. 1 below). As we will argue in this paper the smaller, negative root $\gamma_- = -\nu k^2 - \sqrt{gkA + \nu^2 k^4}$ is the more interesting quantity.

Hide's derivation, based on an original suggestion by Chandrasekhar, was criticized by Reid [25]. We showed [18], however, that by using a variation of that method one can sidestep Reid's criticism and arrive at the same approximate DR shown in Eq. (14) above.

The most extensive comparison of exact and approximate DRs was presented in Willson's seldom-cited paper [26] followed by Menikoff *et al.* [27] who limited their comparison to γ_+ only and who, like Willson, found good agreement between exact and approximate γ_+. Considering γ_-, however, Willson reported gross discrepancies. The exact DR not only disagreed with the approximate γ_-, but there were cases, most notably when $\mu_1 = \mu_2$, where a second exact root did not even exist. In Ref. [22] we also reported that an exact second root (associated with Z_2 in Ref. [22]) did not exist for $k < (\frac{g}{\nu^2})^{1/3}$. Although a second exact root exists for $k > (\frac{g}{\nu^2})^{1/3}$ (see the last paragraph in [22]), we merely noted its existence and did not compare it with the approximate γ_-. A comparison is presented in this paper (Figs. 2 and 3) and indeed there are vast discrepancies between the exact (where it exists) and approximate results.

One would naturally think that the exact result is the correct one. However, recently, in studying the viscous RM instability, we reported [28] that the exact EV result leads to the wrong growth for $\eta(t)$ and that the approximate γ_- which we had used earlier gave the correct behavior. In fact, we reported (without proof—the proof is given in Appendix A of this paper) that the asymptotic RM value is given by

$$\eta(\infty) = \eta_0 + \frac{\dot\eta_0}{2\nu k^2}, \tag{17}$$

and that this is exact for *any* value of μ_1 and μ_2. The above result was obtained [18] by using the approximate eigenvalue γ_-, in contrast to using the exact eigenvalue which misses the mark by more than a factor of 2! The work presented in this paper was spurred in part by this apparent contradiction.

The solution to the above-mentioned puzzle (approximate γ_- gives better results for RM than the exact γ_-) lies in the following basic observation which is also the core conclusion of this paper: The time evolution of the amplitude $\eta(t)$ is given by solving the NS equations as an IV problem [29,30]. In the linear regime it has the general form given by Eq. (1). The EV solution addresses the following question: Are there exponentially growing solutions? The existence of such solutions does not guarantee, nor contradict, the solution in the form of Eq. (2). There are initial conditions, which we have denoted by $\dot\eta_0^{\text{critical}}$, where an initial perturbation decays to zero even in a highly unstable system. As Prosperetti has shown (Eq. (24) in Ref. [30]), the IV approach asymptotes to $\eta(t) \sim e^{\gamma_+ t}$, where γ_+ is the largest root of the DR, but the coefficient is not necessarily the same as in Eq. (2). The two approaches, EV and IV, yield the same $\eta(t)$ for the inviscid case but not for the viscous case.

The IV solution was given by Carrier and Chang [29] explicitly for the case of a single viscous fluid which is case A, Eq. (13a). Prosperetti [30] gave the formal solution in terms of a Laplace transform for the general case and gave an explicit expression only for case B, Eq. (13b). In this paper we derive (Appendix B) the explicit expressions for cases C and D as defined by Eqs. (13c) and (13d).

A second motive for studying cases C and D is that other models [31,32] predict no viscous slowdown when only one of the fluids is viscous; they require viscosity in *both* fluids for any viscous slowdown. While numerical simulations support our approximate model, an exact solution for cases C and D would be further confirmation that viscosity in only one of the fluids is sufficient for slowdown.

In Sec. II we present the DRs for cases C and D and discuss the RT and RM problems in Secs. II A and II B, respectively, comparing exact and approximate growth rates $\gamma_\pm$. In Sec. III we present exact and explicit expressions for $\eta(t)$ as an IV solution for cases C and D, taking up the RT and RM problems in Secs. III A and III B, respectively. A comparison between EV and IV treatments is given in Sec. IV where we use concepts based on $\dot\eta_0^{\text{critical}}$ to propose a hybrid model intermediate between the approximate and the

exact results. We also discuss the dependence on the viscous Atwood number A_μ and point out the existence, in general, of "isogrowth wave numbers," two different wave numbers sharing the same growth rate γ_+. Conclusions and future work are discussed in Sec. V. In two appendices we present the mathematical derivations of our results.

II. EIGENVALUES

A. Rayleigh-Taylor (RT)

The general DR for obtaining exact growth rates [17,20,21,26,27,30] can be written as

$$\gamma^2 + \Lambda(\gamma)\gamma - gkA = 0, \tag{18}$$

with $\Lambda(\gamma)$ given in Appendix A. The complexity of $\Lambda(\gamma)$ rules out any analytic solution for the general case where both $\mu_1 \neq 0$ and $\mu_2 \neq 0$ and they are arbitrary. Here we outline the derivation for case C where $\mu_1 = 0$ and only the heavy fluid has an arbitrary viscosity μ_2. Our notation follows mostly Chandrasekhar's [17] which was also adopted in Ref. [22].

The heavy fluid of density ρ_2 lies in $y \geqslant 0$ and has a perturbed velocity $W = A_2 e^{-ky} + B_2 e^{-q_2 y}$ while the lighter fluid of density ρ_1 lies in $y \leqslant 0$ and has a perturbed velocity $W = A_1 e^{ky}$ (for the general case where $\mu_1 \neq 0$ one would add $B_1 e^{q_1 y}$.) Here

$$(q_{1,2})^2 \equiv k^2 + \gamma \frac{\rho_{1,2}}{\mu_{1,2}}, \tag{19}$$

and $q_{1,2}$ are defined as having a positive real part because the velocity perturbations must vanish as $y \to \pm\infty$.

For the general case the four constants A_1, B_1, A_2, B_2 must be determined by the following four conditions all applied at the interface (see [17] or [22]): (1) a "jump" condition assuring continuity of pressure; (2) continuity of W; (3) continuity of the derivative $DW \equiv dW(y)/dy$; and (4) continuity of $\mu(D^2 + k^2)W(y)$. For case C which has only three constants, A_1, A_2 and B_2, one must give up one of these constraints, and it is the third condition, continuity of DW, that must be given up. Since DW is proportional to the tangential velocity [17], giving it up means allowing for slip at the interface. The same is true for the completely inviscid case $\mu_1 = \mu_2 = 0$. All other conditions, in particular condition (4), are satisfied in all cases.

The procedure is well known and we will not give any more details: The three conditions for the three unknowns are written in matrix form $MV = 0$ with the vector $V = (A_1\ A_2\ B_2)^T$ and the DR is given by setting $\det(M) = 0$ necessary for a nontrivial solution. The result is

$$D(Z) = Z^4 + 2AZ^2 - 2(1 + A)Z + 1 - AQ_2 = 0, \tag{20}$$

where

$$Z \equiv q_2/k \quad \text{and} \quad Q_2 \equiv g/\nu_2^2 k^3. \tag{21}$$

The same result is obtained by taking the limit $\mu_1 \to 0$ in the general DR (Eq. (113) in Chap. X of Ref. [17]). We went through the exercise outlined in this and the preceding paragraph to identify which constraint must be given up when one of the fluids has vanishing viscosity as in case C.

For case D, Eq. (13d), where the heavier fluid has $\mu_2 = 0$, the result is similar:

$$Z^4 - 2AZ^2 - 2(1 - A)Z + 1 - AQ_1 = 0, \tag{22}$$

where

$$Z \equiv q_1/k \quad \text{and} \quad Q_1 \equiv g/\nu_1^2 k^3. \tag{23}$$

For physical applications viscous fluids are usually heavier so case C is probably more useful, for example, honey supported by water.

By using the definitions given by Eqs. (19) and (21) or (23), one obtains the growth rates γ by solving the quartic equations (20) or (22) and using the largest solution for Z. Note that Z's are functions of A and Q_2 or Q_1 only. Now, quartic equations are solved by writing them as a pair of quadratic equations [23]. Note that Eqs. (20) and (22) are relatively simpler forms of quadratic equations as they lack a cubic (Z^3) term. As we hinted above setting $A = 1$ ($\rho_1 = 0$) reproduces the simplest case of all, case A, a single viscous fluid: Eq. (20) above reduces to $Z^4 + 2Z^2 - 4Z + 1 - Q_2 = 0$ which is Eq. (20) in Ref. [22]. Note that when $\rho_1 = \mu_1 = 0$ then $\nu_2 = \nu$; hence $Q_2 = Q$.

The four solutions to Eq. (20) mirror the ones discussed in Ref. [22]. There are two real and two complex solutions for Z. The two complex roots labeled $Z_{3,4}$ have negative real parts and hence are not acceptable. The largest root Z_1 is always positive and hence always present and must be associated with γ_+. As for Z_2, it is real and negative and hence unacceptable if $AQ_2 > 1$, meaning if $k < (\frac{gA}{\nu_2^2})^{1/3}$. However, for $k > (\frac{gA}{\nu_2^2})^{1/3}$, Z_2 is positive and hence acceptable, and the associated γ may be identified with γ_-—more on this later.

Given the complexity of the exact solutions for even a case as simple as case C, the simplicity of the approximate solution, Eq. (14), is even more appreciable. Comparing Eqs. (14) and (18), the approximation corresponds to letting $\Lambda \to 2\nu k^2$ for any and all cases. This approximate solution has the highly desirable property that its viscous term persists even when only one of the fluids is viscous. As we mentioned in the Introduction, this brings up another motivation for studying cases C and D, cases where one of the fluids is inviscid yet viscous effects clearly persist because the other fluid is viscous. We have pointed out [28] that models where all viscous effects vanish as soon as one of the fluids becomes inviscid are rather unphysical and must be limited to cases, like case B, where both fluids have comparable viscosities.

To compare exact and approximate growth rates we follow the usual scaling procedure of reducing the six variables in $\gamma(\rho_1,\ \rho_2,\ \mu_1,\ \mu_2,\ g, k)$ to three nondimensional variables in $Y(A, A_\mu, X)$. We will concentrate on case C; hence $A_\mu = 1$. For X, we define $X \equiv k(\frac{\nu_2^2}{g})^{1/3}$, and for Y we define $Y \equiv \gamma(\frac{\nu_2}{g^2})^{1/3}$. Similar variables were used in Refs. [17,22]. In Fig. 1 we plot Y as a function of X for $A = 0.1$, 0.5, and 1.0, the last one reverting to case A. The agreement between exact and approximate γ_+ is indeed impressive.

In Ref. [22] the same quantities, Y vs X, were plotted for $A = 1$ (Fig. 2 of Ref. [22]). Unfortunately we had made an error in plotting the approximate curve in that figure—the factor of 2 that appears in the approximate Eq. (14) above

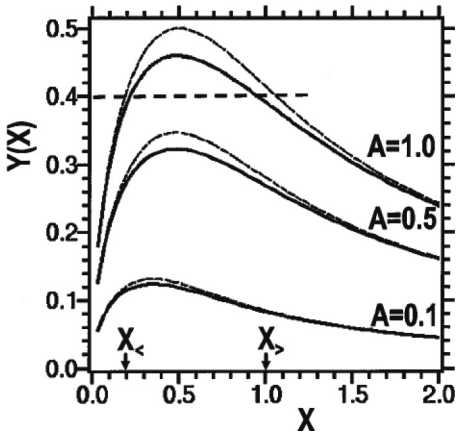

FIG. 1. Y vs X, the normalized growth rate Y defined as $\gamma(\frac{\nu_2}{g^2})^{1/3}$ vs normalized wave number X defined as $k(\frac{\nu_2^2}{g})^{1/3}$, for three values of the Atwood number: $A = 0.1$, 0.5, and 1.0. This is case C, $A_\mu = 1$ ($\mu_1 = 0$). The continuous thick lines are exact results calculated from the first solution Z_1 of Eq. (20) and related to Y by $Y = X^2(Z^2 - 1)$. The dashed lines are approximate results from Eq. (16). This figure is for the larger growth rate γ_+. The flat horizontal dashed line, intersecting the $A = 1.0$ curve, illustrates "isogrowth" rates where Y is the same at $X = X_<$ and $X = X_>$, the subscripts $<$ and $>$ indicating values less than and greater than, respectively, $X_{\max}(\approx \frac{1}{2})$ defined as the location where Y has its maximum value $Y_{\max}$. Isogrowth modes are discussed in Sec. IV D.

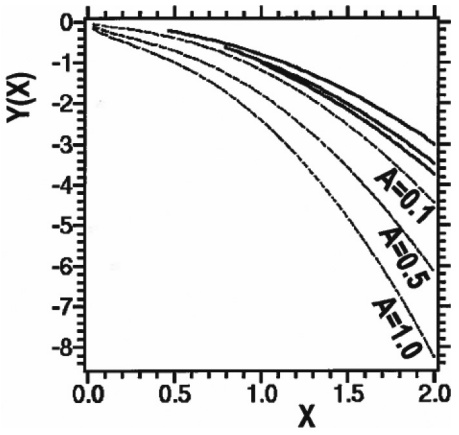

FIG. 2. Same as Fig. 1 for the smaller growth rate γ_-. The exact solutions, from the second solution Z_2 of Eq. (20), exist for $X > A^{1/3}$. The continuous and dashed lines are similarly ordered.

was left out leading to an approximate curve that actually corresponds to $\nu/2$ instead of ν as it should have been. This error was first reported in Ref. [11]. The correct comparison is given in Fig. 1 of this paper and the upper pair of the curves for $A = 1$ in the present Fig. 1 should replace the incorrect Fig. 2 of Ref. [22].

In addition to the generally good agreement between γ_+^{exact} and $\gamma_+^{\text{approx.}}$, we see another property in Fig. 1: All the curves in it are concave downwards. We conclude that $Y(X)$ or, equivalently, $\gamma_+(k)$ has a maximum value $\gamma_+^{\max}$ at some $k = k_{\max}$. It also follows that for any $\gamma_+ < \gamma_+^{\max}$ there are always two wave numbers, call them $k_<$ and $k_>$, which have the *same* growth rate. An example is indicated in Fig. 1. We call them isogrowth wave numbers and will return to these modes in Sec. IV.

A more extensive comparison [27] of exact and approximate γ_+ shows that they agree to within 10% for *any* case. We concentrated on case C because its exact DR is a quartic equation solvable analytically for all four roots.

As Willson reported [26], the same cannot be said of the smaller (and negative, i.e., decaying) growth rate. This is shown in Fig. 2 where we plot Y vs X for the smaller, γ_- root of Eq. (18), using Z_2, the second root of Eq. (20). Z_2 is real, but is positive only for $X > A^{1/3}$; hence the corresponding exact Y start at $X = 0.464$, 0.794, and 1.0 for $A = 0.1$, 0.5, and 1.0, respectively. Unlike Fig. 1, in Fig. 2 there is more than a factor of 2 difference between the exact (continuous lines) and approximate (dashed lines) results.

The difference between γ_-^{exact} and $\gamma_-^{\text{approx.}}$ may not appear important because both are negative and hence represent decaying modes. However, two puzzles remain: First, what should one do when γ_-^{exact} does not exist [26]? Second, why does γ_-^{exact} give such poor results compared with $\gamma_-^{\text{approx.}}$ when they are used in the treatment of the RM instability [28]? In Sec. IV we will propose a solution to these (related) puzzles.

B. Richtmyer-Meshkov (RM)

Following Richtmyer [3] we consider the case of an ideal single shock and set $g = 0$ after shock passage. The approximate DR, Eq. (14), reads $\gamma^2 + 2\nu k^2\gamma = 0$, from which $\gamma_+ = 0$, $\gamma_- = -2\nu k^2$. Equation (2) reduces to [18]

$$\eta(t) = \eta_0 + \dot{\eta}_0 \frac{(e^{\gamma_- t} - 1)}{\gamma_-} = \eta_0 + \dot{\eta}_0 \frac{(1 - e^{-2\nu k^2 t})}{2\nu k^2}. \quad (24)$$

We now turn to the exact DR given by Eq. (18) with $g = 0$. It reads $\gamma^2 + \Lambda(\gamma)\gamma = 0$. Clearly, $\gamma = 0$ is a solution and we conclude that $\gamma_+ = 0$ is actually an exact result valid for *any* value of μ_1 and μ_2 [28]. The other root, γ_-, requires solving $\gamma + \Lambda(\gamma) = 0$ which again cannot be carried out in the general case. Hence we turn to the exact DR given by Eq. (20) for case C. The same treatment applies to the DR for case D given in Eq. (22).

Now, Eq. (20) can be written as

$$(Z - 1)[Z^3 + Z^2 + (1 + 2A)Z - 1] - AQ_2 = 0, \quad (25)$$

and, since $Q_2 = 0$ for $g = 0$, it follows that $Z = 1$ is one root from which $\gamma_+ = 0$, as expected. The remaining three roots are determined by the cubic equation,

$$Z^3 + Z^2 + (1 + 2A)Z - 1 = 0. \quad (26)$$

Again, two of the roots, Z_3 and Z_4, are complex conjugate roots sharing a negative real part, but the third, Z_2, is a real solution from which one obtains $\gamma_-^{\text{exact}} = (Z_2^2 - 1)\nu_2 k^2$. Cubic equations being straightforward to solve we will not write down Z_2 explicitly but note that it is less than 1; hence $\gamma_-^{\text{exact}} < 0$.

With $g = 0$ we cannot use the nondimensional variables X and Y adopted in the previous RT subsection. The Atwood number A being the only variable appearing in Eq. (26) the Z's depend only on A and therefore $\gamma_-^{\text{exact}}/\nu_2 k^2$ depends only on A.

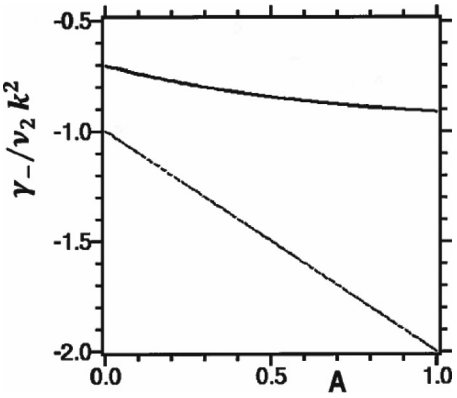

FIG. 3. Exact (thick continuous line) and approximate (dashed) results for the RM instability, $g = 0$, case C. We plot the smaller growth rate γ_- normalized by $\nu_2 k^2$ vs Atwood number A, obtained from Eqs. (26) and (27) which are exact and approximate, respectively. We do not plot the larger growth rate γ_+ because both treatments yield $\gamma_+ = 0$ when $g = 0$.

Similarly for $\gamma_-^{\text{approx.}}$, since $\mu_1 = 0$ for case C it follows that $\nu \equiv (\mu_2 + \mu_1)/(\rho_2 + \rho_1) = \mu_2/(\rho_2 + \rho_1) = \nu_2(1 + A)/2$ and therefore

$$\gamma_-^{\text{approx.}} = -2\nu k^2 = -\nu_2 k^2(1 + A). \tag{27}$$

We conclude that $\gamma_-/\nu_2 k^2$ depends only on A for both exact and approximate treatments, as required also by a simple dimensional argument.

In Fig. 3 we plot $\gamma_-/\nu_2 k^2$ vs Atwood number A for both approximate and exact treatments. As in the RT problem (Fig. 2) they differ by factors of $\sim$2. To illustrate, for $A = 1$ the value of the approximate $\gamma_-/\nu_2 k^2$ is -2 [see Eq. (27)] while the exact result is $-2[4 + (\sqrt{297} - 17)^{\frac{1}{3}} - (\sqrt{297} + 17)^{\frac{1}{3}}] \approx -0.9126$. This value was used in a summary report by Bakhrakh *et al.* [33]. Yet, as reported in [28], numerical simulations of the viscous RM instability clearly favor $\gamma_-^{\text{approx.}}$ over γ_-^{exact}. Similarly, for case B where we provided an exact analytic expression for $\eta(t)$, we found it much closer to the approximate result reproduced here as Eq. (24).

III. INITIAL-VALUE APPROACH

In the preceding section we found eigenvalues, i.e., modes growing like $e^{\gamma_\pm t}$, with exact and approximate expressions for $\gamma_\pm$. The existence of these modes, however, does not guarantee that Eq. (2) is correct in all cases. The evolution of the amplitude must be found by solving the initial-value problem, considered in this section, first for the RT problem and then for the RM problem, following a general discussion applicable to both.

In the linear regime, to which this paper is limited, the general expression is given by Eq. (1) which depends on the suppressed parameters of the system. There are nine such parameters: η_0, $\dot{\eta}_0$, ρ_1, ρ_2, μ_1, μ_2, g or ΔV, k, and t. By dimensional considerations, they can be reduced to five nondimensional parameters. We write Eq. (1) in a "growth factor" form:

$$\frac{\eta(t)}{\eta_0} = f\left(\frac{\dot{\eta}_0}{\eta_0 \nu k^2},\ A, A_\mu,\ \text{Re}; \tau\right), \tag{28}$$

in which the Reynolds number Re is defined by

$$\text{Re} = \text{Re}^{\text{RT}} \equiv \frac{\sqrt{|gA|}}{\nu k^{3/2}} \tag{29a}$$

and

$$\text{Re} = \text{Re}^{\text{RM}} \equiv \frac{|\Delta V A|}{\nu k} \tag{29b}$$

for RT and RM, respectively (see also Ref. [28]). Note that g and ΔV appear explicitly only in the Reynolds numbers. We use the products gA and $\Delta V A$ because the acceleration and the jump velocity always appear multiplied by the Atwood number A. As usual, Re measures the ratio of inertial forces ($\sim g$ or ΔV) to viscous forces ($\sim \nu$).

There are two ways to nondimensionalize time: The first is $\tau \equiv t\sqrt{gkA}$ and $\tau \equiv t|\Delta V k A|$ for RT and RM, respectively. The second way is to use $\tau \equiv \nu k^2 t$ for both RT and RM. The ratio of the two ways is the Reynolds number Re. We will use whichever is convenient; for example, when we want to display results for finite ν as well as for $\nu = 0$ then the first way is obviously more convenient.

To illustrate the above approach consider our approximate model for RT; by substituting $\gamma_\pm$ from Eq. (14) into Eq. (2) we obtain

$$\frac{\eta^{\text{approx.}}(t)}{\eta_0} = e^{-\tau}\left\{\cosh(\tau\sqrt{1 + \text{Re}^2}) + \left(1 + \frac{\dot{\eta}_0}{\eta_0 \nu k^2}\right) \times \frac{\sinh(\tau\sqrt{1 + \text{Re}^2})}{\sqrt{1 + \text{Re}^2}}\right\}, \tag{30}$$

where $\tau = \nu k^2 t$ and $\text{Re} = \text{Re}^{\text{RT}}$. Comparing this expression with Eq. (28) note that neither A nor A_μ appear explicitly in it, a property on which we comment in the concluding section.

The restriction to the linear regime implies that, first, the nondimensional variable $\eta_0 k$ cannot appear in Eq. (28) and that, second, $\frac{\dot{\eta}_0}{\eta_0 \nu k^2}$ must appear only linearly in it.

By choosing $\nu \equiv (\mu_2 + \mu_1)/(\rho_2 + \rho_1)$ as our primary viscous parameter we stress the symmetry between μ_1 and μ_2. All the terms appearing in Eq. (28) are symmetric under the interchange $\mu_1 \leftrightarrow \mu_2$, except for A_μ. Approximate expressions are indeed symmetric [see Eq. (14)] and do not involve A_μ. Exact expressions, however, are not quite symmetric and do depend on A_μ—compare, for example, Eqs. (20) and (22) for $A_\mu = +1$ and -1, respectively. This asymmetry will be studied below.

The time evolution of the growth factor $\eta(t)/\eta_0$ for RT and RM problems will be presented in Secs. III A and III B, respectively.

A. Rayleigh-Taylor (RT)

The exact, general evolution equation for $\eta(t)$ is obtained by inverting the following equation [30]:

$$\tilde{\eta}(s) = \frac{1}{s}\left(\eta_0 + \frac{\eta_0 gkA + \dot{\eta}_0 s}{s^2 + s\Lambda(s) - gkA}\right), \tag{31}$$

where $\tilde{\eta}(s)$ is the Laplace transform of $\eta(t)$:

$$\tilde{\eta}(s) \equiv \int_0^\infty \eta(t) e^{-st} dt, \tag{32}$$

and $\Lambda(s)$ is the same function appearing in Eq. (18) and given explicitly in Appendix A. Its complexity again rules out any analytic solutions for the general $\mu_{1,2}$ case.

For the inviscid case $\mu_1 = \mu_2 = 0$ we have $\Lambda = 0$ and Eq. (31) reduces to

$$\tilde{\eta}(s) = \frac{s\eta_0 + \dot{\eta}_0}{s^2 - gkA}, \tag{33}$$

which, when Laplace inverted, gives the classical solution shown in Eq. (6). For the viscous case, if we use the approximate relation $\Lambda \approx 2\nu k^2$ then the resulting equation can again be Laplace inverted and leads to Eq. (2) with the approximate $\gamma_\pm$ [write the denominator appearing in Eq. (31) as $(s - \gamma_+)(s - \gamma_-)$ and use partial fractions].

Exact analytic expressions for $\eta(t)$ have been given in the literature [29,30] only for cases A and B specified by Eqs. (13a) and (13b). Before we present the results for cases C and D let us quote the exact result for the *asymptotic* value of $\eta(t)$ given by Prosperetti [30]:

$$\eta(t)_{t\to\infty} = \frac{\eta_0\left(\frac{gkA}{\gamma}\right) + \dot{\eta}_0}{2\gamma + \Lambda(\gamma) + \gamma\Lambda'(\gamma)} e^{\gamma t}, \tag{34}$$

where $\gamma \equiv \gamma_+$, the largest real root of the exact DR given in Eq. (18). Since the exact and approximate γ_+ are quite close (see Fig. 1) Eq. (34) implies that the time dependence of the asymptotic growth $\eta \sim e^{\gamma_+ t}$ is well captured by the approximate formula, but the coefficients may differ. We will return to this point later.

In the Appendix we derive the exact, fully explicit result for case C:

$$\frac{\eta(t)}{\eta_0} = \frac{\mathrm{erfc}(\sqrt{\tau_2})}{2 - \frac{AQ_2}{2(1+A)}} + \sum_{i=1}^{4} \frac{Z_i}{D'(Z_i)}\left[\frac{AQ_2}{Z_i^2 - 1} + \frac{\dot{\eta}_0}{\eta_0 \nu_2 k^2}\right] \times e^{(Z_i^2-1)\tau_2}\mathrm{erfc}(-Z_i\sqrt{\tau_2}), \tag{35}$$

where erfc is the complimentary error function $1 - \mathrm{erf}$, $\tau_2 \equiv \nu_2 k^2 t = (\frac{\mu_2}{\rho_2})k^2 t$, and, as before [Eq. (21)], $Q_2 \equiv g/\nu_2^2 k^3$. The Z_i are the four roots of the equation $D(Z) = 0$ where

$$D(Z) \equiv Z^4 + 2AZ^2 - 2(1+A)Z + 1 - AQ_2 \tag{36}$$

and

$$D'(Z) \equiv 4Z^3 + 4AZ - 2(1+A). \tag{37}$$

Note that Eq. (36) is the same as Eq. (20). The roots Z_i, $i = 1 - 4$, are functions of A and Re only because

$$AQ_2 = \frac{gA}{\nu_2^2 k^3} = [(1+A)\mathrm{Re}/2]^2, \tag{38}$$

where $\mathrm{Re} = \mathrm{Re}^{\mathrm{RT}}$ as defined in Eq. (29a).

We recover the single-fluid case, case A, by setting $A = 1$ in the above equations: After some algebra Eq. (35) reduces to the result given in Ref. [29] (note that Carrier and Chang set $\dot{\eta}_0 = 0$.)

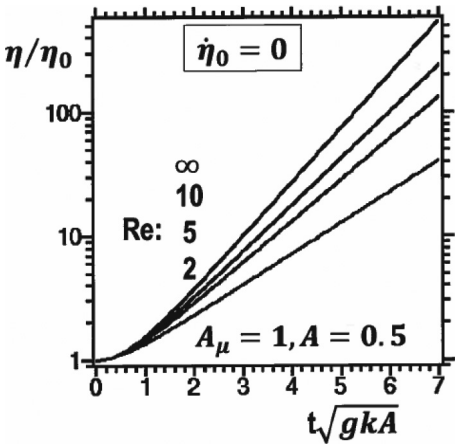

FIG. 4. The RT growth factor $\eta(t)/\eta_0$ as a function of the nondimensional time $t\sqrt{gkA}$ for case C, $A_\mu = 1$, starting with $\dot{\eta}_0 = 0$. The Atwood number A is kept fixed at $A = 0.5$ and four values for the Reynolds number [Eq. (29a)] are considered: $\mathrm{Re} = \mathrm{Re}^{\mathrm{RT}} = 2$, 5, 10, and ∞. These are exact results based on Eq. (35).

A similar expression is obtained for case D:

$$\frac{\eta(t)}{\eta_0} = \frac{\mathrm{erfc}(\sqrt{\tau_1})}{2 - \frac{AQ_1}{2(1-A)}} + \sum_{i=1}^{4} \frac{Z_i}{D'(Z_i)}\left[\frac{AQ_1}{Z_i^2 - 1} + \frac{\dot{\eta}_0}{\eta_0 \nu_1 k^2}\right] \times e^{(Z_i^2-1)\tau_1}\mathrm{erfc}(-Z_i\sqrt{\tau_1}), \tag{39}$$

where $\tau_1 \equiv \nu_1 k^2 t = (\frac{\mu_1}{\rho_1})k^2 t$ and $Q_1 \equiv g/\nu_1^2 k^3$. The Z_i are the roots of $D(Z) = 0$ where

$$D(Z) = Z^4 - 2AZ^2 - 2(1-A)Z + 1 - AQ_1 \tag{40}$$

and

$$D'(Z) = 4Z^3 - 4AZ - 2(1-A). \tag{41}$$

The above equations can also be obtained by noting that to go from case C to case D we can let $\rho_1 \leftrightarrow \rho_2$, $\mu_2 \to \mu_1$, and $g \to -g$; therefore $A \to -A$ and $AQ_2 \to AQ_1$.

In Fig. 4 we plot the growth factor $\eta(t)/\eta_0$ for case C using Eq. (35). We keep the Atwood number fixed at $A = 0.5$ and vary $\mathrm{Re}^{\mathrm{RT}}$ from low ($\mathrm{Re} = 2$, lowest curve in Fig. 4) to high ($\mathrm{Re} = \infty$, highest curve in Fig. 4). For the x axis we chose the nondimensional $\tau = t\sqrt{gkA}$, also called "e-folding time," because it is the same for all Re. A nontrivial check is to verify that the curve plotted for $\mathrm{Re} = \infty$, obtained from Eq. (35) for $\mathrm{Re} \gg 1$, is also the same as the classical curve given by Eq. (6).

From Fig. 4 we see that after 7 e-foldings the exact growth factors for $\mathrm{Re} = 2$, 5, 10, and ∞ are 41, 133, 239, and 548[$= \cosh(7)$], respectively. As expected, the approximate formula given by Eq. (2) with $\gamma_\pm = -\nu k^2 \pm \sqrt{gkA + \nu^2 k^4}$ overestimates the growth giving 55, 186, 310, and 548, respectively. Although these values are some 30%–40% larger than the exact results they are justified, we believe, by the simplicity of the approximate formula. Furthermore, the approximate formula can be used for *any* case, meaning any values of μ_1 and μ_2, so that it should be compared not just

with Eq. (35) but with Eq. (31), the more general Laplace transform which cannot be inverted analytically. Of course that equation can be inverted numerically, in which case the exact, explicit formulas presented in this paper, Eqs. (35) and (39), can serve as highly nontrivial checks of that numerical inversion.

An improved, hybrid model will be presented in Sec. IV C. It consists of using Eq. (2) with $\gamma_+ = \gamma_+^{\rm exact}$ while retaining the relation $\gamma_- = -gkA/\gamma_+$. The exact, approximate, and hybrid results will be compared in that subsection also.

B. Richtmyer-Meshkov (RM)

In the classic calculations of Richtmyer [3] and experiments of Meshkov [4] the fluid velocity is constant after the passage of the shock, leading to growth linear in time. However, as we pointed out earlier [19], this is not necessary: The shock can be followed by acceleration, deceleration, or any general motion as indeed happens in ICF implosions [6,19,34]. The shock induces an initial growth rate $\dot\eta_0 = \eta_0 \Delta V k A = \pm \eta_0 \nu k^2 {\rm Re}^{\rm RM}$; hence Eq. (28) reads

$$\frac{\eta(t)}{\eta_0} = f(\pm {\rm Re}^{\rm RM},\ A_\mu,\ A,\ {\rm Re}^{\rm RT}; \tau), \tag{42}$$

with the Reynolds numbers defined by Eqs. (29a) and (29b).

In the pure RM case we set $g = {\rm Re}^{\rm RT} = 0$ in the above equation and use either $\tau = t|\Delta V k A|$ (inviscid) or $\tau = \nu k^2 t$ (viscous). Equation (31) is much simplified for this case:

$$\tilde\eta(s) = \frac{1}{s}\left(\eta_0 + \frac{\dot\eta_0}{s + \Lambda(s)}\right). \tag{43}$$

However, this Laplace transform still cannot be inverted analytically because of the nontrivial form of $\Lambda(s)$. For the inviscid case $\Lambda = 0$ and one obtains $\eta(t) = \eta_0 + \dot\eta_0 t$ as mentioned above. For the viscous case, if we approximate $\Lambda \approx 2\nu k^2$ then we obtain the result given in Ref. [18] reproduced here as Eq. (24). An *exact* expression for case B was given in Ref. [28]. Exact expressions for cases A, C, and D will be given below after a brief discussion of our approximate expression for viscous RM, Eq. (24).

Using Eq. (8) for $\dot\eta_0$ and ${\rm Re}^{\rm RM}$ defined in Eq. (29b), Eq. (24) can be written as

$$\begin{aligned}\frac{\eta(t)}{\eta_0} &= 1 + \left(\frac{\dot\eta_0}{\eta_0}\right)\frac{\left(1 - e^{-2\nu k^2 t}\right)}{2\nu k^2} = 1 + \Delta V k A \frac{\left(1 - e^{-2\nu k^2 t}\right)}{2\nu k^2} \\ &= 1 \pm (1 - e^{-2\tau}){\rm Re}^{\rm RM}/2,\end{aligned} \tag{44}$$

where $\tau = \nu k^2 t$. The sign is determined by the direction of the shock: positive if it proceeds from a light fluid to a heavy fluid ($A\Delta V > 0$), negative in the opposite case ($A\Delta V < 0$).

In Ref. [28] we claimed, without proof, that the *asymptotic* value of our approximate expression was exact. From the above equation,

$$\eta(t)_{t\to\infty} = \eta_0 + \frac{\dot\eta_0}{2\nu k^2} = \eta_0\left(1 \pm \frac{{\rm Re}^{\rm RM}}{2}\right). \tag{45}$$

To show that the above expression is exact we compare it with the asymptotic value of the exact Laplace transform. From Eq. (43) we obtain

$$\eta(t)_{t\to\infty} = \eta_0 + \frac{\dot\eta_0}{\Lambda(0)}. \tag{46}$$

In Appendix A we show that $\Lambda(0) = 2\nu k^2$ and we conclude that Eq. (45) is exact and valid for arbitrary μ_1 and μ_2. The asymptotic expressions for RT and RM instabilities, given by Eqs. (34) and (45), respectively, are the only explicit and exact results for arbitrary μ_i and ρ_i; all other known exact results fall into one of the four cases listed in Eq. (13).

Note that in the case of the RT instability the effect of viscosity was only a reduction in the growth rate: The amplitude continues to grow exponentially with time, $\eta(t) \sim e^{\gamma t}$, albeit at a reduced rate—see Eq. (34) and Fig. 4. In the case of the RM instability, however, viscosity has a more dramatic effect altering the inviscid growth $\eta(t) \sim t$ to $\eta(t) \to$ constant—see Eq. (45) above and Fig. 5 below.

To investigate exact $\eta(t)$ for arbitrary t we consider first case C, Eq. (13c). Since $g = 0$ for RM, we must set $Q_2 (\equiv \frac{g}{\upsilon_2^2 k^3})$ equal to 0 in Eq. (35). Care, however, must be exercised in evaluating the term $AQ_2/(Z_i^2 - 1)$ for $i = 1$ since $Z_1 = 1$ and numerator and denominator both vanish. We evaluate it using Eq. (25):

$$\begin{aligned}\frac{AQ_2}{Z_1^2 - 1} &= \frac{AQ_2}{(Z_1 + 1)(Z_1 - 1)} \\ &= \left[\frac{Z^3 + Z^2 + (1 + 2A)Z - 1}{Z + 1}\right]_{Z=1} = 1 + A.\end{aligned} \tag{47}$$

Using $D'(1) = 2(1 + A)$, ${\rm erfc}(z) + {\rm erfc}(-z) = 2$, the final result from Eq. (35) is

$$\begin{aligned}\eta(t) = \eta_0 &+ \frac{\dot\eta_0 {\rm erfc}(-\sqrt{\tau_2})}{2(1 + A)\nu_2 k^2} + \frac{\dot\eta_0}{\nu_2 k^2}\sum_{i=2}^{4}\frac{Z_i}{D'(Z_i)} \\ &\times e^{(Z_i^2 - 1)\tau_2}{\rm erfc}(-Z_i\sqrt{\tau_2}),\end{aligned} \tag{48}$$

with $\tau_2 = \nu_2 k^2 t$. The three roots Z_i, $i = 2, 3, 4$, are the roots of $Z^3 + Z^2 + (1 + 2A)Z - 1 = 0$ [see Eq. (26)] and depend only on A.

Figure 5 illustrates the evolution of RM growth factors. Compare with Fig. 4. As discussed above, while viscosity changes the exponential growth of the classical inviscid RT instability to a reduced exponential growth (Fig. 4), it changes the classical inviscid RM growth from linear in time to an asymptotically constant value as seen in Fig. 5.

In the limit $t \to \infty$ only the first and second terms survive in Eq. (48). Although viscosity appears as a product $(1 + A)\nu_2$ in that second term, this is equal to 2ν for case C. Similarly for case D: That product is replaced by $(1 - A)\nu_1$ which is again equal to 2ν, and similarly for case A, the single-fluid case where the product is $2\nu_2 = 2\nu$. Using ${\rm erfc}(-\infty) = 2$ we confirm that $\eta(\infty) = \eta_0 + \dot\eta_0/2\nu k^2$ in all cases, agreeing with Eq. (45).

We end this section by giving the exact, explicit RM expression for the viscous single-fluid case, case A:

$$\begin{aligned}\eta(t) = \eta_0 &+ \frac{\dot\eta_0 {\rm erfc}(-\sqrt{\tau})}{4\nu k^2} + \frac{\dot\eta_0}{\nu k^2}\sum_{i=2}^{4}\frac{Z_i}{D'(Z_i)} \\ &\times e^{(Z_i^2 - 1)\tau}{\rm erfc}(-Z_i\sqrt{\tau}),\end{aligned} \tag{49}$$

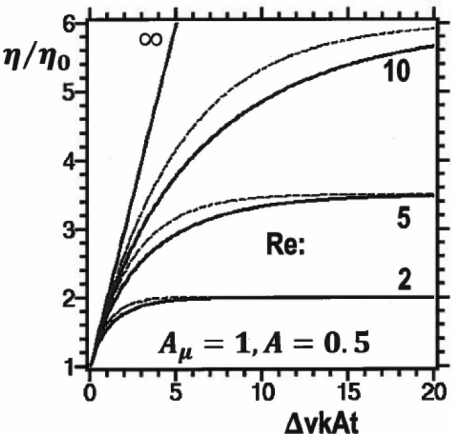

FIG. 5. The RM growth factor $\eta(t)/\eta_0$ as a function of the nondimensional time $\Delta VkAt$ for case C, $A_\mu = 1$. The Atwood number A is kept fixed at $A = 0.5$ and four values for the Reynolds number [Eq. (29b)] are considered: $\mathrm{Re} = \mathrm{Re}^{\mathrm{RM}} = 2$, 5, 10, and ∞. The exact results, using Eq. (48), are shown as thick continuous lines, and approximate results [Eq. (44)] as dashed lines. Both asymptote to $1 + \mathrm{Re}/2$. Compare with Fig. 4.

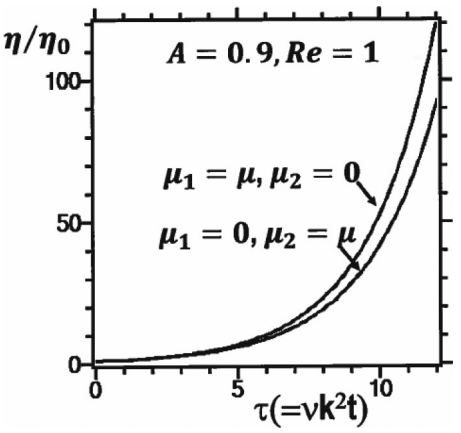

FIG. 6. The RT growth factor $\eta(t)/\eta_0$ vs $\tau \equiv \nu k^2 t$ for $A = 0.9$ and $\mathrm{Re}^{\mathrm{RT}} = 1$. The upper curve has $\mu_1 = \mu$, $\mu_2 = 0$ (hence $A_\mu = -1$) while the lower curve has $\mu_1 = 0$, $\mu_2 = \mu$ (hence $A_\mu = +1$). These are exact results calculated from Eqs. (39) and (35), respectively. The approximate result (not shown) does not distinguish between these two cases and is closer to the upper curve.

where the Z_i are the three roots of the cubic equation $Z^3 + Z^2 + 3Z - 1 = 0$, and $D'(Z) = 4(Z^3 + Z - 1) = -4Z(Z + 2)$. The three roots are $Z_2 = a - b - 1/3$ and $Z_{3,4} = (b - a)/2 - 1/3 \pm i\sqrt{3}(a + b)/2$, where $a \equiv (\frac{2^{1/3}}{3})(\sqrt{297} + 13)^{1/3}$ and $b \equiv (\frac{2^{1/3}}{3})(\sqrt{297} - 13)^{1/3}$. The numerical value of Z_2 is approximately 0.2956 from which the normalized growth rate $\gamma_-/\nu k^2 = Z_2^2 - 1 \cong -0.9126$ as discussed above. This value, however, should *not* be used in the *approximate*, eigenvalue treatment of the RM instability, as we cautioned previously [28].

IV. DEPENDENCE ON A_μ, ASYMPTOTIC DECAY, A HYBRID MODEL, AND ISOGROWTH WAVE NUMBERS

A. Dependence on A_μ

As we have seen, exact results for γ_+ and $\eta(t)$ depend on A_μ : Compare Eq. (20) with Eq. (22) and Eq. (35) with Eq. (39). Even when you set $\nu_1 = \nu_2$ where Eqs. (35) and (39) become (almost) formally identical since $Q_1 = Q_2$, the DRs which give the corresponding Z_i and $D'(Z_i)$, Eqs. (20) and (22), are still different because they call for $A \to -A$. In contrast, the approximate results depend *only* on ν and therefore are always symmetric under $\mu_1 \leftrightarrow \mu_2$.

To accentuate this difference we plot in Fig. 6 $\eta(t)/\eta_0$ vs $\tau \equiv \nu k^2 t$ for $A = 0.9$ and $\mathrm{Re} = \mathrm{Re}^{\mathrm{RT}} = 1$. The two curves in Fig. 6 refer to two different systems: One where only the heavier fluid has viscosity μ (lower curve, $A_\mu = +1$), and one where only the lighter fluid has the same viscosity μ (upper curve, $A_\mu = -1$). Of course ν is the same for both curves. From these two exact curves we conclude that viscosity in the heavier fluid is more effective in suppressing RT growth than the same viscosity appearing in the lighter fluid, although the difference is not very large even at $A = 0.9$; needless to say, the difference is even smaller at lower A. Note that $\nu_1 (= \frac{\mu}{\rho_1})$ is larger than $\nu_2 (= \frac{\mu}{\rho_2})$ because $\frac{\rho_2}{\rho_1} = \frac{1+A}{1-A}$ and ρ_2 is some 19 times larger than ρ_1. This difference between $A_\mu = +1$ and -1 is not captured by the approximate result (not shown) which always overestimates the growth somewhat and is much closer to the upper curve. A hybrid model, presented below, captures the difference.

There is no need to replicate the above exercise for RM instabilities because the difference between the two cases is even smaller and very brief in duration—we know that the exact RM asymptote, Eq. (17), does not depend on A_μ because it involves only ν which is symmetric under $\mu_1 \leftrightarrow \mu_2$.

B. Asymptotic decay and calculation of $\dot{\eta}_0^{\mathrm{crit.}}$

As discussed in the Introduction, one can define $\dot{\eta}_0^{\mathrm{crit.}}$ such that $\eta(t \to \infty) = 0$, called asymptotic decay, in both RT and RM systems. We distinguish this phenomenon from the better-known RM freeze-out where the growth *rate* vanishes instantaneously, i.e., $\dot{\eta} = 0$, and is of a different origin occurring, for example, immediately after a second shock cancels the growth induced by the first shock [19], or if the reflected and transmitted shocks in compressible fluids conspire to arrest the growth of the interface perturbation [35]. Viscosity is not necessary for asymptotic decay or RM freeze-out to occur. As we have seen, the viscous RM instability always ends with freeze-out ($\dot{\eta} = 0$) but not necessarily decay ($\eta = 0$) except for the special case $\mathrm{Re}^{\mathrm{RM}} = 2$ [see Eq. (45)] with the shock proceeding from a heavy to a light fluid, in which case the amplitude decays asymptotically to zero: $\eta(t \to \infty) = \dot{\eta}(t \to \infty) = 0$—see Ref. [18].

Let us point out an interesting contrast between shocked and accelerating systems. A second shock can freeze ($\dot{\eta} = 0$) an amplitude but not when $\eta = 0$ for the simple reason that a shock hitting a flat interface has no effect on it–see Fig. 3(i) in Ref. [19]. In other words one needs a finite amplitude in order to freeze it by a second shock. The opposite is true in an accelerating system: Since the amplitude grows exponentially with time at late times it is not possible to have $\dot{\eta} \to 0$ unless $\eta \to 0$ also.

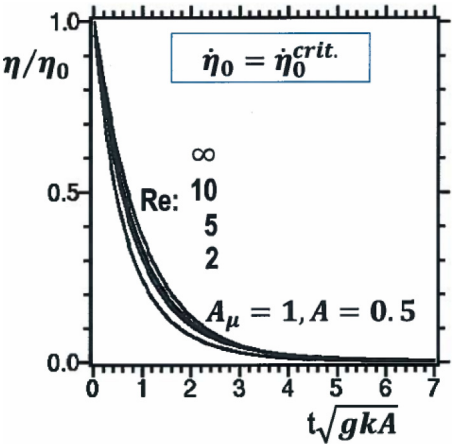

FIG. 7. Same as Fig. 4 with $\dot\eta_0 = \dot\eta_0^{\text{crit.}} = -(\frac{gkA}{\gamma_+})\eta_0$; now the growth factors asymptote to zero.

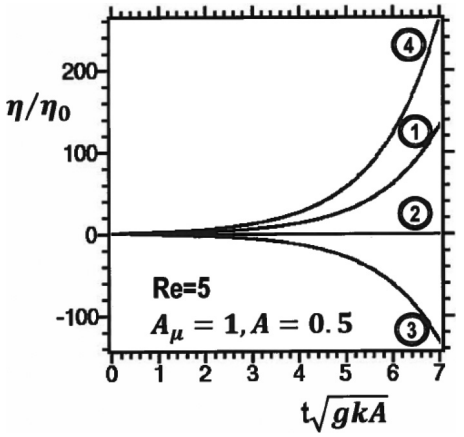

FIG. 8. Variations on $\dot\eta_0$ for the problem displayed in Figs. 4 and 7 with Re = 5. The curve labeled 1 has $\dot\eta_0 = 0$ and is the same as the one appearing in Fig. 4. Curve 2 has $\dot\eta_0 = \dot\eta_0^{\text{crit.}}$ and appears in Fig. 7 also. Curve 3 has $\dot\eta_0 = 2\dot\eta_0^{\text{crit.}}$ and is essentially the negative of curve 1. Curve 4 has $\dot\eta_0 = -\dot\eta_0^{\text{crit.}}$ and is essentially double curve 1. All are exact results using Eq. (35).

The existence of $\dot\eta_0^{\text{crit.}}$ does not depend on viscosity but is more general requiring only that the ratio $F(\infty)/G(\infty)$ be finite—see Eq. (3). As we discussed in the Introduction, using the approximate Eq. (2) one obtains $\dot\eta_0^{\text{crit.}} = \gamma_-\eta_0$. For the classical RT instability given by Eq. (6),

$$\frac{\dot\eta_0^{\text{crit.}}}{\eta_0} = \gamma_- = -\sqrt{gkA} = -gkA/\gamma_+, \tag{50}$$

where $\gamma_+ \equiv \sqrt{gkA}$ is the classic inviscid RT growth rate. What is somewhat surprising is that the *same* combination, gkA/γ_+, appears in the coefficient of the *exact*, *viscous* RT asymptote, Eq. (34), which implies that if $\dot\eta_0 = -\eta_0(\frac{gkA}{\gamma_+})$ then there is no asymptotic growth. We conclude that Eq. (50) is a rather general relationship valid for both inviscid and viscous fluids and for any value of ρ_i and μ_i. Of course γ_+^{exact} is a more complicated quantity than the classic $\sqrt{gkA}$, being the largest real root of Eq. (18), the exact DR for the viscous RT instability.

We illustrate by repeating the same exact RT calculations displayed in Fig. 4 but now, instead of starting with $\dot\eta_0 = 0$, we start with $\dot\eta_0 = \dot\eta_0^{\text{crit.}} = -\eta_0 gkA/\gamma_+$. The new results are displayed in Fig. 7. All amplitudes go to zero at late times. Of course the curve for Re $= \infty$ is given by the classical result, Eq. (6). The rest use Eq. (35). Note that, since this is an RT system, when we choose $\dot\eta_0 = \dot\eta_0^{\text{crit.}}$ then $\eta \to 0$ with $\dot\eta \to 0$, meaning that the amplitude approaches zero with zero slope, as confirmed by the curves in Fig. 7.

We should caution, however, that these situations are rather precarious and a slight deviation from the criticality condition $\dot\eta_0 = \dot\eta_0^{\text{crit.}}$ can lead to large growth, positive or negative. To the two cases $\dot\eta_0 = 0$ and $\dot\eta_0 = \dot\eta_0^{\text{crit.}}$ discussed so far one can add two more: $\dot\eta_0 = 2\dot\eta_0^{\text{crit.}}$ and $\dot\eta_0 = -\dot\eta_0^{\text{crit.}}$. These four cases are shown in Fig. 8 as curves labeled 1, 2, 3, and 4, respectively. Overshooting the targeted value by a factor of 2 ($\dot\eta_0 = 2\dot\eta_0^{\text{crit.}}$, curve 3) takes us back to the growing $\dot\eta_0 = 0$ curve, curve 1, except it is now negative. Of course $\dot\eta_0 = -\dot\eta_0^{\text{crit.}}$, curve 4, has the "wrong" sign (it is positive in value) and ends up essentially doubling the $\dot\eta_0 = 0$ curve, curve 1. Elsewhere we will propose and simulate experiments with $\dot\eta_0^{\text{crit.}}$.

We now turn to the RM instability. It requires only a brief discussion since $\eta(\infty)$ is known exactly [Eq. (45)] and $\eta(\infty) = 0$ only for $\frac{\dot\eta_0}{\eta_0} = \frac{\dot\eta_0^{\text{crit.}}}{\eta_0} = -2\nu k^2$, requiring $\text{Re}^{\text{RM}} = 2$ as mentioned above. This zero asymptote was already discussed in Ref. [18] and all we need to add is that this is an exact result (which we were not aware of at that time).

Stemming from the above considerations of $\dot\eta_0^{\text{crit.}}$, here we would like to propose an alternative relationship between $\gamma_-^{\text{approx.}}$ and γ_-^{exact} which, we believe, solves the conflict between them noted first by Willson [26] and which is clear from our Figs. 2 and 3. Since $q \sim Z$ and we require the real part of $q > 0$ for the eigenvalue analysis [17], in finding the roots of Eq. (18) one must impose this condition and, Willson pointed out, there are cases where only one root (the one we are calling γ_+) can be found [26]. We have verified this explicitly for case A in Ref. [22] (at that time we were not aware of Willson's general analysis). Even when it exists, γ_-^{exact} differs significantly from $\gamma_-^{\text{approx.}}$, as confirmed by Figs. 2 and 3. What we propose is to compare $\gamma_-^{\text{approx.}}$ with a "γ_-^{exact}" *not* associated with Z_2, which may or may not exist, but associated with $\dot\eta_0^{\text{crit.}}$. Specifically, if we define

$$\gamma_-^{\text{exact}} \equiv \dot\eta_0^{\text{crit.}}/\eta_0, \tag{51}$$

then both the approximate and the exact γ_- satisfy the relation

$$\gamma_- = -gkA/\gamma_+. \tag{52}$$

The advantage of this approach is twofold: (i) γ_- always exists because γ_+ does, and (ii) since $\gamma_+^{\text{approx.}} \approx \gamma_+^{\text{exact}}$ (see Fig. 1) we are guaranteed that $\gamma_-^{\text{approx.}} \approx \gamma_-^{\text{exact}}$ defined this way.

We illustrate by comparing $\gamma_-^{\text{approx.}}$ with the new γ_-^{exact} in Fig. 9. The former is given by $\gamma_-^{\text{approx.}} = -gkA/\gamma_+^{\text{approx.}} = -\nu k^2 - \sqrt{gkA + \nu^2 k^4}$ and the latter by $\gamma_-^{\text{exact}} = -gkA/\gamma_+^{\text{exact}}$. Since both $\gamma_-^{\text{approx.}}$ and γ_-^{exact} are given by $-gkA/\gamma_+$, the good agreement between them stems from the proximity of $\gamma_+^{\text{approx.}}$ to γ_+^{exact} seen in Fig. 1.

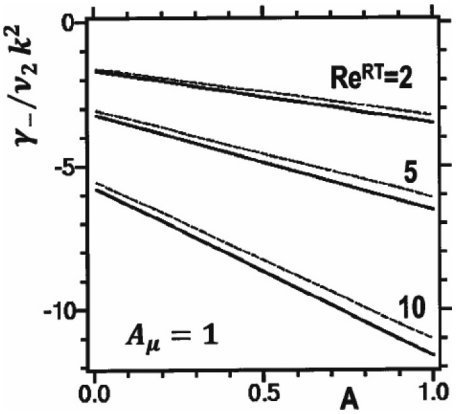

FIG. 9. The smaller, normalized RT growth rate $\gamma_-/\nu_2 k^2$ for case C, $A_\mu = 1$, as a function of the Atwood number A for three values of the Reynolds number $\mathrm{Re}^{\mathrm{RT}} = 2,\ 5$, and 10. We use $\gamma_- = -gkA/\gamma_+$ for both exact (solid lines) and approximate (dashed) results based on $\gamma_+^{\mathrm{exact}}$ and $\gamma_+^{\mathrm{approx.}}$, respectively.

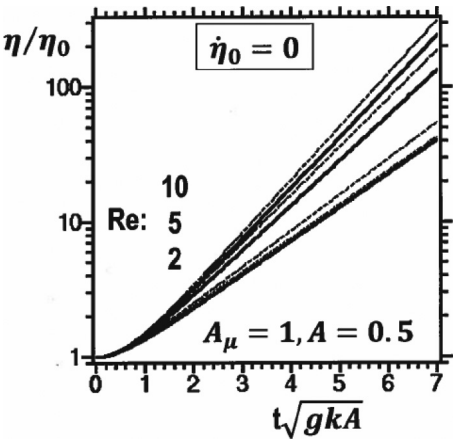

FIG. 10. Comparison of exact, approximate, and hybrid models for the case $A_\mu = 1$, $A = 0.5$, and $\mathrm{Re} = \mathrm{Re}^{\mathrm{RT}} = 2,\ 5$, and 10. Nine curves are displayed in this figure. The exact results (thick continuous lines) are based on Eq. (35). The hybrid results (dotted) use Eq. (2) with $\gamma_+ = \gamma_+^{\mathrm{exact}}$ and $\gamma_- = -gkA/\gamma_+$; they can be barely distinguished from the exact results. The approximate results (dashed) use the same equations with $\gamma_+ = \gamma_+^{\mathrm{approx.}} = -\nu k^2 + \sqrt{gkA + \nu^2 k^4}$; they overestimate the growth factor by 30%–40% after 7 e-foldings.

In summary, we advocate defining $\gamma_-^{\mathrm{exact}}$ not as the second root of the exact DR which may or may not exist, but as $-gkA/\gamma_+^{\mathrm{exact}}$ which always exists. In this way both the exact and the approximate treatment allow $\eta(t)$ to decay to zero (Fig. 7) when $\dot\eta_0 = \dot\eta_0^{\mathrm{crit.}} = \gamma_-\eta_0$. This approach suggests that the simple approximate treatment may be improved leading to a hybrid model discussed in the next subsection.

C. Hybrid model

The exact evolution of $\eta(t)$ is obtained by inverting the Laplace transform given in Eq. (31) which, in general, must be carried out numerically: As far as we know only the four cases listed in Eq. (13) admit analytic solutions. Even then the resulting exact expressions are quite complex—compare Eq. (35), which involves error functions of a complex variable Z, with the approximate result given by Eq. (2) which involves only exponentials with $\gamma_+ \equiv -\nu k^2 + \sqrt{gkA + \nu^2 k^4}$ and $\gamma_- \equiv -gkA/\gamma_+$. Since this $\gamma_+^{\mathrm{approx.}}$ is actually an upper bound for $\gamma_+^{\mathrm{exact}}$(see Ref. [21]) it is not surprising that the approximate results overestimate the growth as we discussed in Sec. III A.

The hybrid model improves upon the approximate model albeit at some cost which we deem worthwhile. It is the *same* as the approximate model, Eq. (2), in which $\gamma_- = -gkA/\gamma_+$ as before, but $\gamma_+ = \gamma_+^{\mathrm{exact}}$, a quantity that must be found from Eq. (18). Except for the four cases listed in Eq. (13) where that DR becomes a quartic equation solvable analytically [23], this root must be found numerically. Needless to say the advantage of the hybrid model is that it does not require Laplace transforms.

It is straightforward to show that our approximate solution, Eq. (2), obeys the following ordinary differential equation (ODE):

$$\ddot\eta(t) - (\gamma_+ + \gamma_-)\dot\eta(t) + \gamma_+\gamma_-\eta(t) = 0. \tag{53}$$

Since $\gamma_+\gamma_- = -gkA$ the above ODE can be written as

$$\ddot\eta(t) - \left(\gamma_+ - \frac{gkA}{\gamma_+}\right)\dot\eta(t) - gkA\eta(t) = 0, \tag{54}$$

and the only difference between the approximate and hybrid solutions is whether one uses the approximate γ_+ from Eq. (16) or the exact γ_+ by solving Eq. (18).

We now return to the exact results displayed in Fig. 4 and compare them with the approximate and the hybrid results for $\mathrm{Re} = \mathrm{Re}^{\mathrm{RT}} = 2$, 5, and 10. We do not consider $\mathrm{Re} = \infty$ since all give the same exact classical evolution for inviscid fluids. This comparison is presented in Fig. 10; the hybrid results are so close to the exact results that they can be barely distinguished. After 7 e-foldings the (exact, hybrid) growth factors are (41, 43), (133, 137), and (239, 243) for Re = 2, 5, and 10, respectively, compared with the approximate results (dashed curves in Fig. 10) which are some 30%–40% larger.

The one and only price to pay in going from the approximate to the more accurate hybrid model for RT is the computation of $\gamma_+^{\mathrm{exact}}$. Since $\gamma_+^{\mathrm{exact}}$ depends on A_μ it differentiates between $A_\mu = +1$ and $A_\mu = -1$, cases C and D, as shown in Fig. 6. The exact growth factors η/η_0 at the end ($\tau = 12$) of the two problems shown in Fig. 6 for $A_\mu = 1$ and -1 are 92 and 121, respectively. The approximate model gives 123 for both cases, while the more accurate hybrid model gives 96 and 121, respectively.

We now examine a system that is not covered by any of the four cases listed in Eqs. (13a)–(13d) and hence the exact solution must be obtained by numerically inverting Eq. (31). Choose $\dot\eta_0 = 0$, $A = 1/6$, $A_\mu = 2/3$, $\tau = \nu k^2 t$, and $\mathrm{Re} = \mathrm{Re}^{\mathrm{RT}} = 2.5$ or 1. These are the only variables needed to compute the growth factor $\eta(t)/\eta_0$ as indicated in Eq. (28). The approximate, hybrid, and exact results are shown in Figs. 11(a) and 11(b) for Re = 2.5 and 1, respectively, showing the expected slowdown with decreased Re.

A concrete system with the above parameters is the following: Oil ($\rho = 1$ g/cm^3, $\mu = 10$ P) and syrup ($\rho = 1.4$ g/cm^3, $\mu = 50$ P) in Earth's gravity, $g = 980$ cm/s^2. This gives $\nu = 25$ S. Re = 2.5 for $k \approx 0.347$ cm^{-1} or $\lambda \approx$

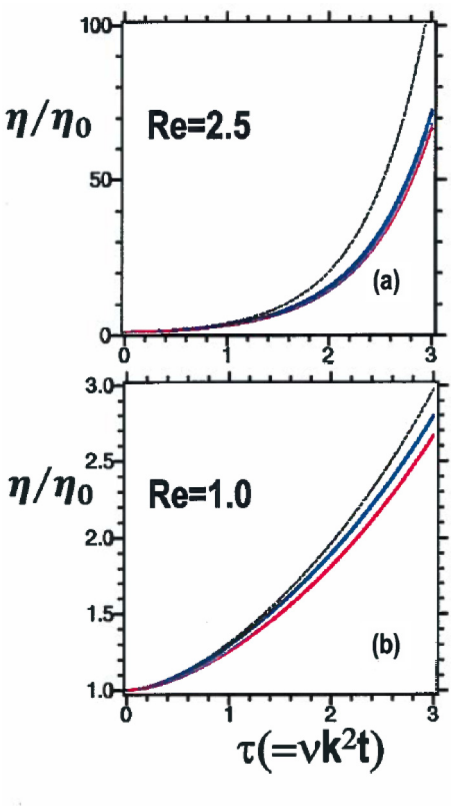

FIG. 11. Growth factors for the case $A_\mu = 2/3$, $A = 1/6$, and $\mathrm{Re}^{\mathrm{RT}} = 2.5$ (a) or 1.0 (b), starting with $\dot{\eta}_0 = 0$. The horizontal axis is $\tau \equiv \nu k^2 t$. Exact, hybrid, and approximate results are plotted as red solid lines, blue solid, and black dashed lines, respectively. This is a case not covered by any of the four special cases listed in Eqs. (13a)–(13d) and exact results must be found numerically using Eq. (31). The exact (red) lines display least growth, while the approximate (black) lines display most growth. The hybrid (blue) lines are intermediate and much closer to the exact results.

18 cm. The classical inviscid growth rate would be $\gamma^{\mathrm{class}} \approx 7.53\ \mathrm{s}^{-1}$, while the viscous approximate rate, from Eq. (16), is $\gamma^{\mathrm{approx.}} \approx 5.10\ \mathrm{s}^{-1}$, somewhat larger, as expected, than the exact viscous rate $\gamma^{\mathrm{exact}} \approx 4.61\ \mathrm{s}^{-1}$, calculated numerically from Eq. (18). Since $\nu k^2 \approx 3\ \mathrm{s}^{-1}$, it follows that $t \approx 1$ s by $\tau \approx 3$ in Fig. 11(a), when the growth factor is about 70. That growth factor reaches only 2.7 for $\mathrm{Re} = 1$ in Fig. 11(b). Now, the simplest way to change $\mathrm{Re}^{\mathrm{RT}}$ is to change g, gravity, leaving everything else the same. Reducing g by a factor of $2.5^2 = 6.25$ reduces Re to 1. It follows that the *same* experiment described here, done on the surface of the Moon, will follow Fig. 11(b) due to its reduced gravity, and the growth rates will be given by $\gamma^{\mathrm{class}} \approx 3.01\ \mathrm{s}^{-1}$, $\gamma^{\mathrm{approx.}} \approx 1.25\ \mathrm{s}^{-1}$, and $\gamma^{\mathrm{exact}} \approx 1.17\ \mathrm{s}^{-1}$. In all cases the hybrid model, which uses γ^{exact} instead of $\gamma^{\mathrm{approx.}}$, gives results closer to the more accurate but numerically obtained growth factors. An alternative and more common method to change g and hence $\mathrm{Re}^{\mathrm{RT}}$ is to carry out microgravity experiments as, for example, in Ref. [36].

The reader may inquire whether the approximate model for RM can be similarly improved, "hybridized." The answer is no, because of two facts: First, $\gamma_+^{\mathrm{approx.}} = \gamma_+^{\mathrm{exact}} = 0$ already. Second, $\gamma_-^{\mathrm{approx.}} = -2\nu k^2$ already gives the exact asymptotic value because $\Lambda(0) = 2\nu k^2$ is an exact relationship, proved in our Appendix A. It is somewhat ironic that the RM model presented in Ref. [18] was better than the RT model on which it was based, though we were not aware of it at that time. The first exact $\eta(t)$ for viscous RM was given in Ref. [28] for case B, and in this paper for cases A, C, and D. That our exact and approximate expressions for RM show good agreement with each other in all cases is due to the two facts mentioned here.

D. Isogrowth wave numbers

As we pointed out earlier and illustrated in Fig. 1, for any $\gamma < \gamma_+^{\max}$ one can find two wave numbers which have the same growth rate. We call these isogrowth wave numbers.

Let us define $k_{\max}$ as that unique value of k where $\gamma = \gamma_{\max} \equiv \gamma_+^{\max}$. Then the isogrowth wave numbers $k_\lessgtr$ come in pairs, one on each side of $k_{\max}$, with $k_< < k_{\max}$ and $k_> > k_{\max}$. As usual, explicit expressions can be found only if we use the approximate treatment, and they are

$$k_< = \frac{gA}{4\nu\gamma} - \sqrt{\frac{g^2A^2}{16\nu^2\gamma^2} - \frac{\gamma}{2\nu}} \tag{55a}$$

and

$$k_> = \frac{gA}{4\nu\gamma} + \sqrt{\frac{g^2A^2}{16\nu^2\gamma^2} - \frac{\gamma}{2\nu}}, \tag{55b}$$

where γ is any growth rate $0 < \gamma < \gamma_{\max}$ shared by the two wave numbers. The above expressions follow from the approximate DR, Eq. (14), viewed not as a quadratic equation in γ but in k. Note that the product $k_< k_> = \gamma/2\nu$. In this approximation $\gamma_{\max}$ and $k_{\max}$ are given by setting $k_< = k_> = k_{\max}$; i.e., $k_{\max} = \frac{gA}{4\nu\gamma_{\max}} = \frac{1}{2}(\frac{gA}{\nu^2})^{1/3}$ and $\gamma_{\max} = \frac{1}{2}(\frac{g^2A^2}{\nu})^{1/3}$.

Perturbations with isogrowth wave numbers have the same asymptotic growth rates but always evolve somewhat differently because now the other growth rate, γ_-, is different between the two: $\gamma_- = -gkA/\gamma_+$ and having the same γ_+ at two different k's implies that γ_- is different between the two. Note that it is not possible to have "isodecay wave numbers" having the same γ_- because the curves for γ_-, which is negative, are not concave but, starting from 0, decrease monotonically with k—see Fig. 2. What this implies is that, in general, even though perturbations of $k_<$ and $k_>$ will share the same γ_+, the corresponding amplitudes will not evolve similarly; i.e., $\eta(t)_{k_<} \neq \eta(t)_{k_>}$. An additional condition is required to achieve $\eta(t)_{k_<} \approx \eta(t)_{k_>}$.

We illustrate with an example. Take $\rho_1 = 1\,\mathrm{g/cm}^3$, $\rho_2 = 3\,\mathrm{g/cm}^3$; hence $A = 1/2$. Let $\mu_1 = 0$ and $\mu_2 = 1$ P, hence $\nu = \frac{1}{4}$ S. Taking $g = 1000\ \mathrm{cm/s}^2$, we find $\gamma_{\max} = 50\ \mathrm{s}^{-1}$ at $k = k_{\max} = 10\ \mathrm{cm}^{-1}$. Suppose we seek $\gamma = 40\ \mathrm{s}^{-1}$; then the two $k-$ values are $k_< \approx 3.77\ \mathrm{cm}^{-1}$ ($\lambda \approx 1.7$ cm) and $k_> \approx 21.2\ \mathrm{cm}^{-1}$ ($\lambda \approx 0.3$ cm). The decaying modes are $\gamma_-(k_<) \approx -47\ \mathrm{s}^{-1}$ and $\gamma_-(k_>) \approx -265\ \mathrm{s}^{-1}$. These modes decay quickly; nevertheless, the corresponding $\eta(t)$, starting with $\dot{\eta}_0 = 0$, are still different, as shown in Fig. 12(a). The mode with $k = k_>$ grows about 1.6 times more than the other, even though its Re is about 13 times smaller. The exact results,

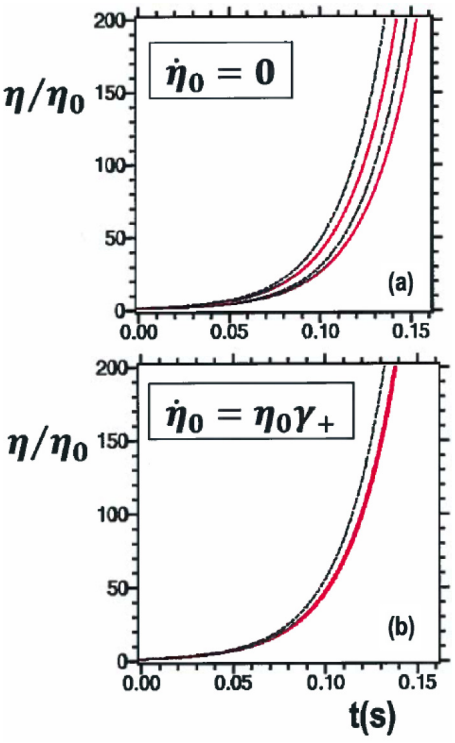

FIG. 12. Growth factor $\eta(t)/\eta_0$ in a system where $\rho_1 = 1$ g/cm^3, $\rho_2 = 3$ g/cm^3, $\mu_1 = 0$, $\mu_2 = 1$ P, and $g = 1000$ cm/s^2, plotted as a function of time in seconds for two isogrowth wave numbers: $k = k_< \approx 3.8$ cm^{-1} and $k = k_> \approx 21.2$ cm^{-1}, which share the same growth rate $\gamma_+ = 40$ s^{-1} (see text). In the top figure (a) $\dot\eta_0 = 0$ and the $k_>$ mode grows faster in both the exact treatment (solid red lines) and the approximate treatment (dashed black lines). In the bottom figure (b) $\dot\eta_0 = \eta_0\gamma_+$ and the two $k_<$ and $k_>$ modes collapse into one for both treatments [there are four curves in panel (b) also]. With $\dot\eta_0 = \eta_0\gamma_+$ the evolution is purely exponential $e^{\gamma_+ t}$ with the same γ_+ at the two widely separated wave numbers $k_<$ and $k_>$—see the dashed horizontal line in Fig. 1. We do not show hybrid results because they are indistinguishable from the exact results.

calculated from Eq. (35), are also shown, in red: Again, the $k_>$ mode grows about 1.5 times more than the $k_<$ mode. Equation (35) is too complicated to throw light on this issue, but the approximate Eq. (2) gives (setting $\dot\eta_0 = 0$ and neglecting $e^{\gamma_- t}$ terms)

$$\eta(t)/\eta_0 \approx \frac{e^{\gamma_+ t}}{1 - \gamma_+/\gamma_-}, \tag{56}$$

explaining the factor of 1.6 by

$$\frac{(1 - \gamma_+/\gamma_-)_{k_<}}{(1 - \gamma_+/\gamma_-)_{k_>}} = \frac{1 + \frac{40}{47}}{1 + \frac{40}{265}} \approx 1.6. \tag{57}$$

Still neglecting $e^{\gamma_- t}$ terms but now keeping the $\dot\eta_0$ term Eq. (2) gives

$$\eta(t)/\eta_0 \approx \left(\frac{\frac{\dot\eta_0}{\eta_0} - \gamma_-}{\gamma_+ - \gamma_-}\right) e^{\gamma_+ t}, \tag{58}$$

so that if $\frac{\dot\eta_0}{\eta_0} = \gamma_+$ then $\eta(t)/\eta_0 \approx e^{\gamma_+ t}$ and the two modes indeed evolve identically. This is the required additional condition, as shown in Fig. 12(b). We conclude that isogrowth wave numbers are necessary but not sufficient to have $\eta(t)$ be the same at two different wave numbers; one must also have $\frac{\dot\eta_0}{\eta_0} = \gamma_+$, their shared growth rate. As usual, this is another condition that can be satisfied by starting the instability with appropriately tuned shocks.

V. REVIEW, CONCLUDING REMARKS, AND FUTURE WORK

(i) In this paper we introduced the viscous Atwood number A_μ to classify various cases and compared approximate, exact, and hybrid treatments of the viscous RT and RM instabilities. We believe that exact explicit expressions can be obtained only for the four cases (13a)–(13d); other cases require solving Eq. (18) and inverting Eq. (31) or Eq. (43), all done numerically, as we did for the example presented in Fig. 11.

The approximate result uses Eq. (2) with the approximate DR given in Eq. (14). The hybrid model also uses Eq. (2) but with γ_+, the larger growth rate, obtained from the exact DR, Eq. (18), and $\gamma_- = -gkA/\gamma_+$. This last condition ensures that for any inviscid or viscous case one can always find a critical initial growth rate $\dot\eta_0^{\text{crit.}} = \gamma_-\eta_0 = -(\frac{gkA}{\gamma_+})\eta_0$ such that the amplitude, instead of growing exponentially with time, will decay exponentially to zero.

These three approaches, exact, approximate, and hybrid, were illustrated in Figs. 10 and 11. Since asymptotically $\eta(t) \sim e^{\gamma_+ t}$ the difference between γ_+^{exact} and $\gamma_+^{\text{approx.}}$ can naturally result in large differences after several e-foldings, as seen in Fig. 10. The hybrid model, as expected, performs much better: In Fig. 10 exact and hybrid methods can be barely distinguished at Re $= 2$ and not at all at Re $= 5$ and 10. At higher Re the differences are even less noticeable since all three approaches lead to the classical inviscid evolution given in Eq. (6).

We believe the hybrid model presented in this paper and the approximate method presented in Ref. [18] solve the quest undertaken by Prosperetti in Ref. [30]. After presenting the Laplace transform of the exact solution Prosperetti searched for a model that approximated the exact result, but he did not find one: He found models that agreed with the asymptotic behavior of $\eta(t)$ but violated the initial conditions, and models that captured the initial conditions but violated the asymptotic evolution—see his Figs. 1–3. The hybrid model fulfills both conditions and, to a lesser degree, so does the approximate model, Eq. (2). By construction, Eq. (2) accommodates arbitrary initial conditions and, to the extent that $\gamma_+^{\text{approx.}} \approx \gamma_+^{\text{exact}}$ (see Fig. 1), its asymptotic evolution is also acceptable. By defining $\gamma_- \equiv -gkA/\gamma_+$ and using γ_+^{exact} in Eq. (2) the hybrid model goes one step further reproducing the asymptotic evolution exactly, albeit at the price of finding γ_+^{exact}.

(ii) We discussed that the approximate model is symmetric under $\mu_1 \leftrightarrow \mu_2$ while the hybrid and exact models are not. A similar property is the following: In the Boussinesq approximation [37] one keeps the Atwood number A multiplying the acceleration g or the jump velocity ΔV but otherwise treats the system as one fluid with average densities and viscosities,

i.e., $\rho_{1,2} \to (\rho_1 + \rho_2)/2$ and $\mu_{1,2} \to (\mu_1 + \mu_2)/2$, i.e., set $A = A_\mu = 0$. In the Boussinesq approximation all possible viscous cases collapse into one and the result can be written formally [see Eq. (28)] as

$$\frac{\eta^B(t)}{\eta_0} = f\left(\frac{\dot{\eta}_0}{\eta_0 \nu k^2},\ 0, 0,\ \mathrm{Re}; \tau\right). \tag{59}$$

Note that the Atwood number appears only in Re (=$\mathrm{Re}^{\mathrm{RT}}$ or $\mathrm{Re}^{\mathrm{RM}}$) multiplying g or ΔV. Clearly, in the Boussinesq approximation one uses $\tau = \nu k^2 t$.

Recent considerations of the Boussinesq approximation in the context of RT and RM instabilities can be found in Refs. [38–40]. We pointed out that inviscid linear results remain the same under this approximation, but nonlinear results do not [39]. Here let us point out that *viscous* linear results also remain the same in our *approximate* treatment, but the exact and hybrid results do not remain the same, as the reader can easily verify from the expressions given in this paper.

(iii) Equation (53) can be considered a generalization of Taylor's equation, Eq. (7), which is recovered when $\gamma_+ = \gamma^{class.} = \sqrt{gkA}$. We would like to propose Eq. (53) as a bridge between the eigenvalue and the initial-value formulations of RT instabilities in the presence of viscosity or any other stabilizing mechanism such as ablation, rotation, magnetic fields, etc., as reflected in γ_+.

Additionally, Eq. (53) and its solution, Eq. (2), may describe the time evolution of perturbations in other types of hydrodynamic instabilities such as the Kelvin-Helmholtz instability with or without the stabilizing mechanisms mentioned above. We hope to investigate this possibility in the future.

(iv) From our discussion of isogrowth perturbations it should be clear that this is a general phenomenon not limited to viscosity: *Any* concave curve for γ_+ will admit two different wave numbers $k_<$ and $k_>$ that have the same growth rate γ_+. As another example, one can write the DR for RT with surface tension, which is a quadratic equation in γ (see Ref. [17]), as a cubic equation in k, $k^3 - k_c^2 k + \frac{\gamma^2 k_c^2}{gA} = 0$, and obtain from it the pair $k_<$ and $k_>$ which have the same growth rate γ between 0 and $\gamma_{\max}$ where $\gamma_{\max}^2 \equiv 2gAk_c/3\sqrt{3}$, k_c being the cutoff wave number given by $k_c^2 \equiv (\rho_2 - \rho_1)g/T^{(s)}$. In all cases if one wants to achieve $\eta(t)_{k_<} \approx \eta(t)_{k_>}$ one must further impose the condition $\frac{\dot{\eta}_0}{\eta_0} = \gamma_+$.

(v) To treat the viscous RM instability we followed Richtmyer's incompressible approach: The shock is an impulsive acceleration giving $\dot{\eta}_0 = \eta_0 \Delta V k A$ followed by $g = 0$, an approach whose power should be amply clear to the reader. The exact (but still incompressible) treatment requires Laplace inverting Eq. (43) which, again, we believe can be done analytically only for the four cases A–D mentioned above. For RM there is no distinction between the approximate and a hybrid model because the exact result $\gamma_+ = 0$ is already captured by the approximate model. Furthermore, since $\gamma_-^{\mathrm{approx.}} = -2\nu k^2$ and $\Lambda(0) = 2\nu k^2$ is an exact result (see Appendix A), we are guaranteed that the approximate model gives the correct asymptote, as reported earlier [28]. Exact and approximate RM results were compared in Fig. 5.

Another model for the viscous RM instability can, in limited cases, perform better than our approximate model during the early brief period when approximate and exact results are different. That model [31,32] misses the asymptotic value completely and can in fact go negative at late times [28,41]. At early times it does well for cases where $\mu_1 \approx \mu_2$ but when $\mu_1 \approx 0$ or $\mu_2 \approx 0$ it is completely wrong because it predicts *no* viscous effect. This means that for cases C and D studied in this paper, where there is only one viscous fluid, that model would predict inviscid (!) RM growth. Physical intuition, let alone exact results, lead us to expect that viscosity in only one fluid is sufficient for viscous behavior. A more recent comparison can be found in Ref. [42].

(vi) A similar shortcoming can be found in the nonlinear model of Sohn [43]. This is quite disappointing since the inviscid ingredients of that model have performed well. Sohn [43] built a model for nonlinear bubbles in viscous RT and RM instabilities by adding viscosity to Goncharov's nonlinear, inviscid model [44] which, in turn, was an extension of Layzer's $A = 1$ inviscid model [45]. Although there are more modern, inviscid, nonlinear models [46], Layzer's model and Goncharov's extension of it to arbitrary A have proved highly useful and compared well with numerical simulations, particularly when limited to the bubble part of the instability. Sohn's further extension [43] to viscous fluids was indeed the natural next step. We have performed two-dimensional (2D) numerical simulations (results to be presented elsewhere) showing that Sohn's nonlinear viscous model is acceptable in many cases, but not in others. Its failure is similar to that of Carles and Popinet [31,32] although a completely different technique (originated by Layzer) is used in the nonlinear model. As we have shown [47], Layzer's model can be solved analytically by choosing $\eta_0 = \eta^* \equiv 1/(1 + c)k$ where $c = 1$ for 3D (three-dimensional) and $c = 2$ for 2D perturbations. The same choice solves Sohn's viscous model. We find, however, that for case D, for example, when $\mu_2 = 0$, Sohn's model predicts inviscid evolution for $\eta(t)$ no matter what the value of μ_1, a shortcoming similar to that of Carles and Popinet and a clearly unphysical behavior. This shortcoming does not occur for the single-fluid case, case A, and in Ref. [28] we presented the nonlinear analytic solution for that case. The nonlinear extension to arbitrary Atwood number remains for a future investigation.

(vii) Another application left for the future is the approximate equivalence between viscosity and material strength (denoted by Y), both being properties that suppress growth. We advocated [28] a relationship between these two properties:

$$Y/\mu = 2\sqrt{gkA}/3 \tag{60a}$$

and

$$Y/\mu = 2|\dot{\eta}_0|k/3 \tag{60b}$$

for RT and RM, respectively. In the exact, hybrid, or approximate expressions given in this paper one can replace μ_1 or μ_2 by Y_1 or Y_2 using the above relationships and arrive at formulas describing, approximately, RT or RM growth suppressed by material strength. As discussed in Ref. [28] this is only a crude (but useful—see Ref. [48]) equivalence; hence one need not distinguish between exact, hybrid, and approximate expressions—simple approximate results will do. The equivalence appears to hold up even in nonlinear jet formation [49]. Turbulence generated by RT and RM instabilities have

been studied in detail [50–52] in fluids with no viscosity or strength; questions on how they will be affected by such physical properties are left for the future.

(viii) Finally compressibility which, we believe, is the hardest fluid property to incorporate into RT and RM instabilities, is also left for a future study. At present there is no treatment which parallels Richtmyer's work, albeit for linear perturbations, but which includes compressibility *and* viscosity in even one fluid, let alone two. At present the only available approach is numerical simulations and we hope to present such results in the future; we believe that the already rich and interesting phenomena that occur in RT and RM instabilities are further enriched when fluid properties such as viscosity, strength, and compressibility are taken into account.

ACKNOWLEDGMENT

This work was performed under the auspices of the U. S. Department of Energy by Lawrence Livermore National Laboratory under Contract No. DE-AC52-07NA27344.

APPENDIX A: $\Lambda(\gamma)$ AND $\Lambda(0)$

For completeness we provide the exact expression for $\Lambda(\gamma)$ in Eq. (18). It has the dimensions of a growth rate γ, which appears also in the wave numbers q_1 and q_2 defined in Eq. (19).

$$\Lambda(\gamma) = 4k\frac{N(\gamma)}{D(\gamma)}, \tag{A1}$$

$$N(\gamma) = -\rho_1\rho_2\gamma + k(\mu_2-\mu_1)[\rho_2(k-q_1)-\rho_1(k-q_2)] + k^2(\mu_2-\mu_1)^2(k-q_2)(k-q_1)/\gamma, \tag{A2}$$

$$\mathrm{D}(\gamma) = (\rho_1+\rho_2)[\rho_2(k-q_1)+\rho_1(k-q_2)]. \tag{A3}$$

The above form was given by Prosperetti [30]. For a derivation and early history see Chandrasekhar [17].

Some care must be exercised to show that $\Lambda(0) = 2\nu k^2$, where $\nu \equiv (\mu_2+\mu_1)/(\rho_2+\rho_1)$, because as $\gamma \to 0$ $q_{1,2} \to k$ and there are "0/0" terms. These are evaluated following L'Hôpital's rule using $\frac{\partial q_i}{\partial \gamma} = \frac{\rho_i}{2q_i\mu_i} = \frac{1}{2\nu_i q_i}$. After repeated applications of that rule (we omit the rather lengthy but straightforward steps) one finds $\Lambda(0) = 2\nu k^2$. This completes the proof that the asymptotic RM value $\eta(\infty) = \eta_0 + \dot{\eta}_0/2\nu k^2$ is exact for *any* value of μ_i and ρ_i, as claimed in Ref. [28].

Although Hide adopted a different approach to derive the approximate DR [Eq. (14)] his result is equivalent to letting $\Lambda(\gamma) \to \Lambda(0)$ in the exact DR, Eq. (18). We should point out that the exact DR given in Refs. [17,21], in its standard form, differs from Eq. (18) by multiplicative factors. This is discussed by Menikoff *et al.* [53] who treated the initial-value problem in a general form. In special cases such as $\rho_1 = 0$ or $\mu_1 = 0$ these factors can vanish and the relationship between the two forms becomes ill defined. This was another reason why we went through the standard derivation to arrive at Eqs. (20) and (22), in addition to identifying which constraint (continuity of tangential velocity, i.e., no-slip condition) one must give up when one of the fluids has no viscosity.

Hide's approximation being an upper bound for γ_+, the largest root of the exact DR [21], $\gamma_+^{\text{approx.}}$ may be denoted by γ_+^{upper}. A lower bound γ_+^{lower} is given by another quartic equation (Eq. (11) in Ref. [27]). The closeness of these two bounds (Fig. 2 in Ref. [27]) explains the success of Hide's approximation. One can solve that second quartic equation for γ_+^{lower} and use the average $(\gamma_+^{\text{upper}} + \gamma_+^{\text{lower}})/2$ as an improved estimate for $\gamma_+^{\text{approx.}}$. Successive approximations using Newton's method quickly converge [27], and a first iteration has been recently reported [54].

Finally, one should not underestimate the following usage of Hide's explicit approximation. The exact DR reduces to a quartic equation only for the four cases [Eqs. (13a)–(13d)] discussed in this paper. For the general case the exact DR, $\gamma^2 + \gamma\Lambda(\gamma) - gkA = 0$, must be solved numerically. All numerical techniques for finding the zeros of an expression call for a "first guess" and $\gamma_+^{\text{approx.}}$ provides an excellent one: By trying values slightly less than $\gamma_+^{\text{approx.}}$ one quickly finds the numerical value of γ_+^{exact}, and indeed this was the method we used to find γ_+^{exact} needed in Fig. 11.

APPENDIX B: DERIVATION OF EQ. (35)

We now outline the derivation of Eq. (35) for case C, $\mu_1 = 0$. Equation (39) is derived similarly for case D, $\mu_2 = 0$. These two cases are more general than the single-fluid case A treated in Ref. [29] but more specific than the completely general case (arbitrary μ_1 and μ_2) treated in Refs. [30,54,55] which must be solved numerically.

The general solution, Eq. (22) in Ref. [30], can be written down in terms of its Laplacian transform $\tilde{\eta}(s)$:

$$\tilde{\eta}(s) = \frac{1}{s}\left(\eta_0 + \frac{s\dot{\eta}_0 + gkA\eta_0}{s^2 + s\Lambda(s) - gkA}\right), \tag{B1}$$

where Λ is given by Eq. (23) of Ref. [30] and reproduced here as Eq. (A1) above after replacing the growth rate γ by s, the parameter for the Laplace transform.

Our notation follows mostly that of Carrier and Chang [29] since we are essentially extending their one-fluid treatment to two fluids, plus keeping all $\dot{\eta}_0$ terms. We will perform several checks in the intermediate steps.

Let $\psi_y^i(x,y,t)$ be the stream function in fluid i and assume all x dependence to be given by e^{ikx}; i.e., $\psi^i(x,y,t) = e^{ikx}\psi^i(y,t)$. Denote differentiation with respect to a variable like x, y, or t by the subscript of that variable and $\mathrm{D} \equiv \frac{\partial}{\partial y}$, as in $\nabla^2\psi = \psi_{xx} + \psi_{yy} = (-k^2 + D^2)\psi$.

Momentum conservation reads

$$\nabla^2\psi_t^i = \nu_i\nabla^2\nabla^2\psi^i. \tag{B2}$$

The x and y components of the velocity are given by $\psi_{yy} = D^2\psi$ and $-\psi_{xy} = -ikD\psi$, respectively. Continuity of the normal velocity at the interface reads

$$\eta_t \equiv \dot{\eta} = -\psi_{xy}^1(y=0) = -\psi_{xy}^2(y=0), \tag{B3}$$

i.e., $\dot{\eta} = -ik\psi_y^1 = -ik\psi_y^2$ at $y = 0$.

The tangential stresses must be continuous across the interface. Since

$$\tau_{xy}^i = \mu_i\left[\psi_{yyy}^i - \psi_{xxy}^i\right], \tag{B4}$$

we have

$$\psi^2_{yyy} = \psi^2_{xxy} \quad \text{at} \quad y = 0. \tag{B5}$$

Without surface tension the normal stresses must also be continuous: $-\tau_{yy} = p + 2\mu\psi_{xyy} = p(0,0,t) + \rho\psi_{xt} - \rho g y - \mu[\psi_{xxx} - \psi_{xyy}]$ in each fluid. Remembering that $\mu_1 = 0$ for case C, it follows that at the interface, $y = \eta$,

$$\rho_1\psi^1_{xt} - \rho_1 g\eta = \rho_2\psi^2_{xt} - \rho_2 g\eta - \mu_2\left[\psi^2_{xxx} - \psi^2_{xyy}\right], \tag{B6}$$

which can be written as

$$\rho_2\psi^2_t - \rho_1\psi^1_t + i(\rho_2 - \rho_1)\left(\frac{g}{k}\right)\eta + \mu_2[k^2 + D^2]\psi^2 = 0, \tag{B7}$$

with $\psi^{1,2}$ evaluated at $y = 0$.

We now take the Laplace transform of the above equations, denoting the Laplace transform of a quantity by a tilde ($\sim$) above it. From Eq. (B2) with $\nu_1 = 0$ we have

$$\tilde{\psi}^1 = A^1(s,k)e^{ky}, \tag{B8}$$

while in fluid 2 with $\nu_2 = \mu_2/\rho_2$ Eq. (B2) reads

$$s(D^2 - k^2)\tilde{\psi}^2 - \nu_2(D^2 - k^2)(D^2 - k^2)\tilde{\psi}^2 = 0. \tag{B9}$$

The solution can be written in the following form:

$$\tilde{\psi}^2 = A^2(s,k)e^{-ky} + B^2(s,k)e^{-q_2 y}, \tag{B10}$$

where $q_2 \equiv (k^2 + \frac{s}{\nu_2})^{1/2}$. Since ψ^2 satisfies Eq. (B5) at $y = 0$ the functions A^2 and B^2 are related via the requirement $D(D^2 + k^2)\tilde{\psi}^2 = 0$ at $y = 0$, with the result

$$B^2 = \frac{-2k^3}{q_2\left(2k^2 + \frac{s}{\nu_2}\right)}A^2, \tag{B11}$$

so that Eq. (B10) reads

$$\tilde{\psi}^2(s,k,y) = \left\{e^{-ky} - \frac{2k^3 e^{-q_2 y}}{q_2\left(2k^2 + \frac{s}{\nu_2}\right)}\right\}A^2. \tag{B12}$$

Finally, a relationship between A^1 and A^2 can be found by using Eq. (B3) which reads $\tilde{\psi}^1_y = \tilde{\psi}^2_y$ at $y = 0$, with the result

$$A^2 = -\left(2k^2 + \frac{s}{\nu_2}\right)\left(\frac{\nu_2}{s}\right)A^1. \tag{B13}$$

Substituting (B13) in (B12) we have

$$\tilde{\psi}^2 = \left\{-\left(1 + \frac{2k^2\nu_2}{s}\right)e^{-ky} + \frac{2k^3\nu_2}{sq_2}e^{-q_2 y}\right\}A^1. \tag{B14}$$

Note that $\tilde{\psi}^1$ [Eq. (B8)] and $\tilde{\psi}^2$ [Eq. (B14)] now satisfy continuity of the normal velocity $D\psi$ at $y = 0$, i.e., $D\tilde{\psi}^2 = D\tilde{\psi}^1 = kA^1$, as well as continuity of the tangential stress at $y = 0$ which reads $D(D^2 + k^2)\tilde{\psi}^2 = 0$, for any s, implying any time. These are the same conditions used in the eigenvalue treatment [17].

The next step is to transform Eq. (B7) using $\mathcal{L}[\psi_t(t)] = s\mathcal{L}[\psi(t)] - \psi(t = 0) = s\tilde{\psi} - \psi(0)$. We get

$$\rho_2[s\tilde{\psi}^2 - \psi^2(0,0)] - \rho_1[s\tilde{\psi}^1 - \psi^1(0,0)] + i(\rho_2 - \rho_1)\left(\frac{g}{k}\right)\tilde{\eta} + \mu_2(k^2 + D^2)\tilde{\psi}^2 = 0, \tag{B15}$$

evaluated at $y = 0$. The initial values $\psi^{1,2}(0,0)$ are related to $\dot{\eta}_0 \equiv \dot{\eta}(t = 0)$ from Eq. (B3):

$$\dot{\eta}_0 = -ik\psi^1_y(0,0) = -ik^2\psi^1(0,0) = ik^2\psi^2(0,0), \tag{B16}$$

where $\psi^1(0,0) = -\psi^2(0,0)$ follows from assuming zero initial vorticity.

From Eq. (B8) $\tilde{\psi}^1(y = 0) = A^1$. From Eq. (B14) $\tilde{\psi}^2(y = 0) = \{-1 - 2\frac{k^2\nu_2}{s} + 2\frac{k^3\nu_2}{sq_2}\}A^1(s,k)$ and $(k^2 + D^2)\tilde{\psi}^2(y = 0) = \{-2k^2 - \frac{4k^4\nu_2}{s} + \frac{2k^3}{q_2} + \frac{4k^5\nu_2}{sq_2}\}A^1$. Substituting these expressions in Eq. (B15) we get

$$\left\{-s(\rho_2 + \rho_1) - 4k^2\mu_2 + \frac{4k^3\mu_2}{q_2} - \frac{4k^4\nu_2\mu_2}{s} + \frac{4k^5\nu_2\mu_2}{sq_2}\right\}A^1 = -\frac{i(\rho_2 + \rho_1)\dot{\eta}_0}{k^2} - \frac{ig(\rho_2 - \rho_1)\tilde{\eta}}{k}. \tag{B17}$$

Next, we substitute for $A^1(s,k)$ by transforming Eq. (B3):

$$s\tilde{\eta} - \eta_0 = -ik\tilde{\psi}^1_y(y = 0) = -ik^2A^1. \tag{B18}$$

Substituting Eq. (B18) in Eq. (B17) and collecting terms we have

$$s\tilde{\eta} - \eta_0 = \frac{gkA\eta_0 + s\dot{\eta}_0}{s^2 + 2\nu_2^2(1 + A)k^2(q_2 - k)q_2 - gkA}. \tag{B19}$$

We now pause to compare the above equation with Eq. (B1). Consistency requires that $s\Lambda(s) = 2\nu_2^2(1 + A)k^2(q_2 - k)q_2$, so we study $\Lambda(\gamma)$ given in Eq. (A1) in the limit $\mu_1 \to 0$, meaning $q_1 \to \infty$. In this limit we need keep only terms proportional to q_1 in N and D:

$$N \to -k\mu_2\left[\rho_2 + \frac{k\mu_2(k - q_2)}{s}\right]q_1,$$

$$D \to -\rho_2(\rho_2 + \rho_1)q_1.$$

The q_1 factors in N and D cancel out and $\Lambda = 4kN/D$ is finite and we verify that $s\Lambda(s)$ indeed equals the middle term in the denominator of Eq. (B19). This is an independent, nontrivial check of our calculations at this intermediate stage.

The final stage is to invert Eq. (B19) to find $\eta(t)$. First, note that for the classical inviscid case $\Lambda \to 0$ and the denominator in Eq. (B19) becomes $s^2 - gkA$ (q_2 diverges only as $1/\sqrt{\mu_2}$ while $\nu_2 \sim \mu_2 \to 0$; hence the middle term vanishes). Writing $s^2 - gkA = (s - \gamma_+)(s - \gamma_-)$ with $\gamma_\pm = \pm\sqrt{gkA}$ and using partial fractions, the result of the inversion is Eq. (6). For the viscous case using the approximation $\Lambda(s) = 2\nu k^2 = \text{const.}$, the same procedure leads to Eq. (2) in which $\gamma_\pm$ are given by the two solutions to Eq. (14).

The steps are more complicated with the exact kernel appearing in the denominator of Eq. (B19). We define $Z \equiv \frac{q_2}{k} = (1 + \frac{s}{\nu_2 k^2})^{1/2}$ and write Eq. (B19) as

$$s\tilde{\eta} - \eta_0 = \frac{AQ_2\eta_0 + \left(\frac{s}{\nu_2^2 k^4}\right)\dot{\eta}_0}{Z^4 + 2AZ^2 - 2(1 + A)Z + 1 - AQ_2}, \tag{B20}$$

with $Q_2 \equiv g/\nu_2^2 k^3$ as before [Eq. (21)]. Note that the denominator in the above equation is the same as the left-hand side of Eq. (20) with $\gamma \leftrightarrow s$. In that equation this fourth-order polynomial is set equal to zero because Eq. (20) stands for $\mathrm{Det}(M) = 0$, the condition necessary for solving the set of equations (three in this case, four in the general case) capturing the continuity and other conditions imposed on the eigenfunctions, as is done in a typical eigenvalue problem [17] leading to a dispersion relation like Eq. (20), $D(z) = 0$. Here, however, we set the same polynomial equal to zero for a purely mathematical purpose: We set $Z^4 + 2AZ^2 - 2(1+A)Z + 1 - AQ_2 = 0$ so that we can find its four roots, Z_i, $i = 1-4$, write the polynomial as a product of four factors, and write Eq. (B20) as

$$\tilde{\eta} = \frac{\eta_0}{s} + \frac{\frac{\dot{\eta}_0}{\nu_2^2 k^4} + \frac{AQ_2\eta_0}{s}}{(Z-Z_1)(Z-Z_2)(Z-Z_3)(Z-Z_4)}. \tag{B21}$$

Clearly, $Z_i = Z_i(A, Q_2)$. We do so to use partial fractions,

$$\frac{1}{\prod_{i=1}^4 (Z-Z_i)} = \sum_{i=1}^4 \frac{1}{D'(Z_i)(Z-Z_i)}, \tag{B22}$$

where the derivative $D'(z) = 2(2Z^3 + 2AZ - 1 - A)$. Thus isolated, each term in the sum can be inverted using well-known results from Laplace transforms. The roots satisfy the following relations:

$$\sum_{i=1}^4 \frac{1}{D'(Z_i)} = 0, \tag{B23a}$$

$$\sum_{i=1}^4 \frac{Z_i}{D'(Z_i)} = 0, \tag{B23b}$$

$$\sum_{i=1}^4 \frac{Z_i^2}{D'(Z_i)} = 0, \tag{B23c}$$

and

$$\sum_{i=1}^4 \frac{Z_i^3}{D'(Z_i)} = 1. \tag{B23d}$$

Equation (B21) reads

$$\tilde{\eta} = \frac{\eta_0}{s} + \sum_{i=1}^4 \frac{\frac{\dot{\eta}_0}{\nu_2^2 k^4} + \frac{AQ_2\eta_0}{s}}{D'(Z_i)(Z-Z_i)}. \tag{B24}$$

The inverse of the first term, η_0/s, is simply η_0. In the remaining terms we have to invert expressions like $1/(Z-Z_i)$ and $1/s(Z-Z_i)$, using the definition of Z in terms of s (see above). We use

$$\begin{aligned}\mathcal{L}^{-1}\left(\frac{1}{Z-Z_i}\right) &= k\sqrt{\nu_2}\mathcal{L}^{-1}\left\{\frac{1}{\sqrt{s+\nu_2 k^2} - k\sqrt{\nu_2}Z_i}\right\} \\ &= k\sqrt{\nu_2}e^{-\nu_2 k^2 t}\left\{\frac{1}{\sqrt{\pi t}} + k\sqrt{\nu_2}Z_i e^{\nu_2 k^2 Z_i^2 t}\,\mathrm{erfc}(-k\sqrt{\nu_2}Z_i\sqrt{t})\right\}.\end{aligned} \tag{B25}$$

Note that the first term above, containing $1/\sqrt{\pi t}$, is independent of Z_i and hence will drop out when forming the sum over i and using Eq. (B23a).

Somewhat more complicated is the inversion of $1/s(Z-Z_i)$ terms. Using

$$\mathcal{L}^{-1}\left[\frac{g(s)}{s}\right] = \int_0^t f(u)du, \tag{B26}$$

where $f(t) \equiv \mathcal{L}^{-1}[g(s)]$, we need to integrate over the right-hand side of Eq. (B25), i.e., evaluate an integral of the form

$$I \equiv \int_0^t e^{bu}\mathrm{erf}(a\sqrt{u})du. \tag{B27a}$$

Transforming $\sqrt{u} = x$ and integrating by parts, the result is

$$I = \frac{e^{bt}}{b}\mathrm{erf}(a\sqrt{t}) - \frac{a}{b\sqrt{a^2-b}}\mathrm{erf}(\sqrt{a^2-b}\sqrt{t}). \tag{B27b}$$

Since $\mathrm{erfc}(z) \equiv 1 - \mathrm{erf}(z)$ we have

$$\begin{aligned}\mathcal{L}^{-1}\left[\frac{1}{s(Z-Z_i)}\right] &= k^2\nu_2 Z_i \int_0^t e^{k^2\nu_2(Z_i^2-1)u}[1 - \mathrm{erf}(-k\sqrt{\nu_2}Z_i\sqrt{u})]du \\ &= k^2\nu_2 Z_i\left\{\frac{e^{k^2\nu_2(Z_i^2-1)t} - 1}{k^2\nu_2(Z_i^2-1)} - \int_0^t e^{k^2\nu_2(Z_i^2-1)u}\mathrm{erf}(-k\sqrt{\nu_2}Z_i\sqrt{u})du\right\} \\ &= \frac{Z_i}{Z_i^2-1}\left(e^{k\nu_2(Z_i^2-1)t} - 1\right) + \frac{Z_i}{Z_i^2-1}e^{k^2\nu_2(Z_i^2-1)t}\mathrm{erf}(k\sqrt{\nu_2}Z_i\sqrt{t}) - \frac{Z_i^2}{Z_i^2-1}\mathrm{erf}(k\sqrt{\nu_2}\sqrt{t}).\end{aligned} \tag{B28}$$

Using Eqs. (B25) and (B28) we can now invert Eq. (B24) to obtain

$$\eta(t) = \eta_0 + AQ_2\eta_0 \sum_{i=1}^{4} \frac{1}{D'(Z_i)} \left(\frac{Z_i}{Z_i^2-1}\right) \left[e^{k^2\nu_2(Z_i^2-1)t}\,\mathrm{erfc}(-k\sqrt{\nu_2}Z_i\sqrt{t}) - 1 - Z_i\,\mathrm{erf}(k\sqrt{\nu_2}\sqrt{t})\right]$$
$$+ \frac{\dot\eta_0}{k^2\nu_2} \sum_{i=1}^{4} \frac{Z_i}{D'(Z_i)} e^{k^2\nu_2(Z_i^2-1)t}\,\mathrm{erfc}(-k\sqrt{\nu_2}Z_i\sqrt{t}). \tag{B29}$$

We have used $\mathrm{erfc}(-z) = 2 - \mathrm{erfc}(z) = 1 + \mathrm{erf}(z)$.

As a check, note that Eq. (B24) can be written as

$$s\tilde\eta - \eta_0 = \sum_{i=1}^{4} \frac{AQ_2\eta_0 + s\dot\eta_0/\nu_2^2k^4}{D'(Z_i)(Z - Z_i)}. \tag{B30}$$

The left-hand side of the above equation is the Laplace transform of $\dot\eta(t)$. Therefore

$$\dot\eta(t) = \sum_{i=1}^{4} \frac{1}{D'(Z_i)} \left\{AQ_2\eta_0\mathcal{L}^{-1}\left(\frac{1}{Z-Z_i}\right) + \frac{\dot\eta_0}{\nu_2^2k^4}\mathcal{L}^{-1}\left(\frac{s}{Z-Z_i}\right)\right\}$$
$$= \sum_{i=1}^{4} \frac{Z_i}{D'(Z_i)} \left[AQ_2\eta_0k^2\nu_2 + \left(Z_i^2-1\right)\dot\eta_0\right] e^{k^2\nu_2(Z_i^2-1)t}\,\mathrm{erfc}(-k\sqrt{\nu_2}Z_i\sqrt{t}). \tag{B31}$$

The same result is obtained by differentiating Eq. (B29), using the "sum rules" given in Eqs. (B23a)–(B23d). Integrating the above equation is another way of deriving Eq. (B29).

Equation (B29) can be simplified. The coefficient of the term $\mathrm{erf}(k\sqrt{\nu_2}\sqrt{t})$ is

$$\sum_{i=1}^{4} \frac{Z_i^2}{D'(Z_i)\left(Z_i^2-1\right)} = \sum_{i=1}^{4} \frac{1}{D'(Z_i)\left(Z_i^2-1\right)}, \tag{B32}$$

where we have subtracted and added 1 to the numerator Z_i^2 and used Eq. (B23a). To simplify further we adopt a technique pioneered by Prosperetti [56] and here give only the essential elements for the problem at hand. The basic idea is to factor the sixth-order polynomial $D(Z)(Z^2-1)$. In Prosperetti's notation, $c_i = Z_i$ for $i = 1-4$ and choose $c_5 = -c_6 = 1$. With $D(Z)$ given by Eq. (20) we have $P_{6,5} = 2D(1) = -2AQ_2$ and $P_{6,6} = -2D(-1) = -2[4(1+A) - AQ_2]$. Now, from Ref. [56],

$$0 = S_6(0) = \sum_{i=1}^{6} \frac{1}{P_{6,i}} = \sum_{i=1}^{4} \frac{1}{D'(Z_i)\left(Z_i^2-1\right)} + \frac{1}{P_{6,5}} + \frac{1}{P_{6,6}}, \tag{B33}$$

from which

$$\sum_{i=1}^{4} \frac{1}{D'(Z_i)\left(Z_i^2-1\right)} = \frac{1}{2AQ_2} + \frac{1}{2[4(1+A) - AQ_2]} = \frac{2(1+A)}{AQ_2[4(1+A) - AQ_2]}, \tag{B34}$$

to be used in Eq. (B32).

The last term in Eq. (B29) that can be simplified by this technique is $\sum_{i=1}^{4} \frac{Z_i}{D'(Z_i)(Z_i^2-1)}$, the coefficient of the -1 term in Eq. (B29). We use [56]

$$0 = S_6(1) = \sum_{i=1}^{4} \frac{Z_i}{D'(Z_i)\left(Z_i^2-1\right)} + \frac{Z_5}{P_{6,5}} + \frac{Z_6}{P_{6,6}}, \tag{B35}$$

from which

$$\sum_{i=1}^{4} \frac{Z_i}{D'(Z_i)\left(Z_i^2-1\right)} = -\frac{Z_5}{P_{6,5}} - \frac{Z_6}{P_{6,6}} = -\frac{1}{P_{6,5}} + \frac{1}{P_{6,6}}$$
$$= \frac{1}{2AQ_2} - \frac{1}{2[4(1+A) - AQ_2]} = \frac{2(1+A) - AQ_2}{AQ_2[4(1+A) - AQ_2]}. \tag{B36}$$

The rest of the terms in Eq. (B29) cannot be simplified by Prosperetti's technique because Z_i appears in the exponential as well as the complementary error function erfc. Substituting Eqs. (B32), (B34), and (B36) in Eq. (B29) and collecting terms we

arrive at

$$\frac{\eta(t)}{\eta_0} = \frac{2(1+A)\mathrm{erfc}(k\sqrt{\nu_2 t})}{4(1+A)-AQ_2} + \sum_{i=1}^{4} \frac{Z_i}{D'(Z_i)}\left[\frac{AQ_2}{Z_i^2-1} + \frac{\dot{\eta}_0}{\eta_0 k^2 \nu_2}\right] e^{(Z_i^2-1)k^2\nu_2 t}\mathrm{erfc}(-Z_i k\sqrt{\nu_2 t}), \tag{B37}$$

which is the result given in Eq. (35). It is instructive to set $t = 0$ in the above equation and check that indeed $\eta(t=0) = \eta_0$ and $\dot{\eta}(t=0) = \dot{\eta}_0$, two arbitrary constants of the initial-value problem. Much more work is required to show that the above expression reduces to the inviscid result, Eq. (6), in the limit $\nu_2 \to 0$.

[1] Lord Rayleigh, Investigation of the character of the equilibrium of an incompressible heavy fluid of variable density, *Scientific Papers* (Dover, New York, 1965), Vol. 2.

[2] G. I. Taylor, The instability of liquid surfaces when accelerated in a direction perpendicular to their plane. I, Proc. R. Soc. London, Ser. A **201**, 192 (1950).

[3] R. D. Richtmyer, Taylor instability in shock acceleration of compressible fluids, Commun. Pure Appl. Math. **13**, 297 (1960).

[4] E. E. Meshkov, Instability of the interface of two gases accelerated by a shock wave, Izv. Akad. Nauk SSSR, Mekh. Zhidk. Gaza **5**, 151 (1969).

[5] J. Nuckolls, L. Wood, A. Thiessen, and G. Zimmerman, Laser compression of matter to super-high densities: Thermonuclear (CTR) applications, Nature (London, U. K.) **239**, 139 (1972).

[6] J. D. Lindl, *Inertial Confinement Fusion* (Springer-Verlag, New York, 1998).

[7] L. F. Wang, W. H. Ye, X. T. He, J. F. Wu, Z. F. Fan, C. Xue, H. Y. Guo, W. Y. Miao, Y. T. Yuan, J. Q. Dong *et al.*, Theoretical and simulation research of hydrodynamic instabilities in inertial-confinement-fusion implosions, Sci. China: Phys., Mech. Astron. **60**, 1674 (2017).

[8] H. F. Robey, J. O. Kane, B. A. Remington, R. P. Drake, O. A. Hurricane, H. Louis, R. J. Wallace, J. Knauer, P. Keiter, D. Arnett, and D. D. Ryutov, An experimental testbed for the study of hydrodynamic issues in supernovae, Phys. Plasmas **8**, 2446 (2001).

[9] Y. Zhou, Rayleigh-Taylor and Richtmyer-Meshkov instability induced flow, turbulence, and mixing. I, Phys. Rep. **720–722**, 1 (2017).

[10] Y. Zhou, Rayleigh-Taylor and Richtmyer-Meshkov instability induced flow, turbulence, and mixing. II, Phys. Rep. **723–725**, 1 (2017).

[11] R. E. Rosensweig, Y. Hirota, S. Tsuda, and K. Raj, Study of audio speakers containing ferrofluid, J. Phys.: Condens. Matter **20**, 204147 (2008).

[12] C. Harig, P. Molnar, and G. A. Houseman, Rayleigh-Taylor instability under a shear stress free top boundary condition and its relevance to removal of mantle lithosphere from beneath the Sierra Nevada, Tectonics **27**, TC6019 (2008).

[13] C. R. Weber, D. S. Clark, A. W. Cook, L. E. Busby, and H. F. Robey, Inhibition of turbulence in inertial-confinement-fusion hot spots by viscous dissipation, Phys. Rev. E **89**, 053106 (2014).

[14] T. M. Willey, K. Champley, R. Hodgin, L. Lauderbach, M. Bagge-Hansen, C. May, N. Sanchez, B. J. Jensen, A. Iverson, and T. van Buuren, X-ray imaging and 3D reconstruction of in-flight exploding foil initiation flyers, J. Appl. Phys. **119**, 235901 (2016).

[15] T. G. Theofanous, Aerobreakup of Newtonian and viscoelastic liquids, Annu. Rev. Fluid Mech. **43**, 661 (2011).

[16] A. A. Blinova, M. M. Romanova, and R. V. E. Lovelace, Boundary between stable and unstable regimes of accretion. Ordered and chaotic unstable regimes, Mon. Not. R. Astron. Soc. **459**, 2354 (2016).

[17] S. Chandrasekhar, *Hydrodynamic and Hydromagnetic Stability* (Oxford University Press, London, 1968).

[18] K. O. Mikaelian, Effect of viscosity on Rayleigh-Taylor and Richtmyer-Meshkov instabilities, Phys. Rev. E **47**, 375 (1993).

[19] K. O. Mikaelian, Richtmyer-Meshkov instabilities in stratified fluids, Phys. Rev. A **31**, 410 (1985).

[20] W. J. Harrison, The influence of viscosity on the oscillations of superposed fluids, Proc. Math. Soc. (London) **s2–6**, 396 (1908).

[21] R. Bellman and R. H. Pennington, Effects of surface tension and viscosity on Taylor instability, Q. Appl. Math. **12**, 151 (1954).

[22] K. O. Mikaelian, Rayleigh-Taylor instability in finite-thickness fluids with viscosity and surface tension, Phys. Rev. E **54**, 3676 (1996).

[23] J. V. Uspensky, *Theory of Equations* (McGraw-Hill, New York, 1948), Chap. V.

[24] R. Hide, The character of the equilibrium of an incompressible heavy viscous fluid of variable density: An approximate theory, Proc. Cambridge Philos. Soc. **51**, 179 (1955).

[25] W. H. Reid, The effects of surface tension and viscosity on the oscillations of superposed fluids, Proc. Cambridge Philos. Soc. **57**, 415 (1961).

[26] A. J. Willson, On the stability of two superposed fluids, Proc. Cambridge Philos. Soc. **61**, 595 (1965).

[27] R. Menikoff, R. C. Mjolsness, D. H. Sharp, and C. Zemach, Unstable normal mode for Rayleigh-Taylor instability in viscous fluids, Phys. Fluids **20**, 2000 (1977).

[28] K. O. Mikaelian, Shock-induced interface instability in viscous fluids and metals, Phys. Rev. E **87**, 031003 (2013).

[29] G. F. Carrier and C. T. Chang, On an initial value problem concerning Taylor instability of incompressible fluids, Q. Appl. Math. **16**, 436 (1959).

[30] A. Prosperetti, Motion of two superposed viscous fluids, Phys. Fluids **24**, 1217 (1981).

[31] P. Carles and S. Popinet, Viscous nonlinear theory of Richtmyer-Meshkov instability, Phys. Fluids **13**, 1833 (2001).

[32] P. Carles and S. Popinet, The effect of viscosity, surface tension and non-linearity on Richtmyer-Meshkov instability, Eur. J. Mech. B/Fluids **21**, 511 (2002).

[33] S. M. Bakhrakh, O. B. Drennov, N. P. Kovalov, A. I. Lebedev, E. E. Meshkov, A. L. Mikhailov, N. V. Nevmerzhitsky, P. N. Nozovtsev, V. A. Rayevsky, G. P. Simonov, V. P. Solovyev, and I. G. Zhidov, Hydrodynamic instability in strong media, Lawrence Livermore National Laboratory Report No. UCRL-CR-126710, 1997 (unpublished).

[34] S. Atzeni and J. Meyer-ter-Vehn, *The Physics of Inertial Fusion* (Oxford University Press, Oxford, 2004).

[35] K. O. Mikaelian, Freeze-out and the effect of compressibility in the Richtmyer-Meshkov instability, Phys. Fluids **6**, 356 (1994).

[36] F. Quirion, M.-C. Asselin, and G. G. Ross, Propagation of interfacial waves in microgravity, Chem. Soc. Rev. **23**, 275 (1994).

[37] J. Boussinesq, *Théorie de l'Écoulement Tourbillonnant et Tumultueux des Liquids dans les Lits Rectilignes a Grande Section* (Gauthier-Villars et Fils, Paris, 1897), Vol. 1.

[38] H. G. Lee and J. Kim, A comparison study of the Boussinesq and the variable density models on buoyancy-driven flows, J. Eng. Math. **75**, 15 (2012).

[39] K. O. Mikaelian, Boussinesq approximation for Rayleigh-Taylor and Richtmyer-Meshkov instabilities, Phys. Fluids **26**, 054103 (2014).

[40] N. Schneider and S. Gauthier, Vorticity and mixing in Rayleigh-Taylor Boussinesq turbulence, J. Fluid Mech. **802**, 395 (2016).

[41] K. O. Mikaelian, Comment on "The effect of viscosity, surface tension and non-linearity on Richtmyer-Meshkov instability" [Eur. J. Mech. B Fluids **21**, 511 (2002)], Eur. J. Mech. B/Fluids **43**, 183 (2014).

[42] Y. B. Sun, J. J. Tao, R. H. Zeng, and X. T. He, Effects of viscosity and elasticity on the Richtmyer-Meshkov instability, Phys. Rev. E **98**, 033102 (2018).

[43] S.-I. Sohn, Effects of surface tension and viscosity on the growth rates of Rayleigh-Taylor and Richtmyer-Meshkov instabilities, Phys. Rev. E **80**, 055302 (2009).

[44] V. N. Goncharov, Analytical Model of Nonlinear, Single-Mode, Classical Rayleigh-Taylor Instability at Arbitrary Atwood Numbers, Phys. Rev. Lett. **88**, 134502 (2002).

[45] D. Layzer, On the instability of superposed fluids in a gravitational field, Astrophys. J. **122**, 1 (1955).

[46] Q. Zhang and W. Guo, Universality of finger growth in two-dimensional Rayleigh-Taylor and Richtmyer-Meshkov instabilities at all density ratios, J. Fluid Mech. **786**, 47 (2016).

[47] K. O. Mikaelian, Analytic Approach to Nonlinear Rayleigh-Taylor and Richtmyer-Meshkov Instabilities, Phys. Rev. Lett. **80**, 508 (1998).

[48] A. López Ortega, M. Lombardini, D. I. Pullin, and D. I. Meiron, Numerical simulations of the Richtmyer-Meshkov instability in solid-vacuum interfaces using calibrated plasticity laws, Phys. Rev. E **89**, 033018 (2014).

[49] A.-M. He, J. Liu, C. Liu, and P. Wang, Numerical and theoretical investigation of jet formation in elastic-plastic solids, J. Appl. Phys. **124**, 185902 (2018).

[50] I. W. Kokkinakis, D. Drikakis, D. L. Youngs, and R. J. R. Williams, Two-equation and multi-fluid turbulence models for Rayleigh-Taylor mixing, Int. J. Heat Fluid Flow **56**, 233 (2015).

[51] B. Thornber, D. Drikakis, D. L. Youngs, and R. J. R. Williams, The influence of initial conditions on turbulent mixing due to Richtmyer-Meshkov instability, J. Fluid Mech. **654**, 99 (2010).

[52] M. Hahn, D. Drikakis, D. L. Youngs, and R. J. R. Williams, Richtmyer-Meshkov turbulent mixing arising from an inclined material interface with realistic surface perturbations and reshocked flow, Phys. Fluids **23**, 046101 (2011).

[53] R. Menikoff, R. C. Mjolsness, D. H. Sharp, C. Zemach, and B. J. Doyle, Initial value problem for Rayleigh-Taylor instability of viscous fluids, Phys. Fluids **21**, 1674 (1978).

[54] C. Xie, J. Tao, and J. Li, Viscous Rayleigh-Taylor instability with and without diffusion effect, Appl. Math. Mech. (Engl. Transl.) **38**, 263 (2017).

[55] R. A. Axford, Initial value problems of the Rayleigh-Taylor instability type, Los Alamos Scientific Laboratory Report No. LA-5378, 1973 (unpublished).

[56] A. Prosperetti, Viscous effects on small-amplitude surface waves, Phys. Fluids **19**, 195 (1976).